Research in Astron. Astrophys. **2013** Vol. **13** No. **4**, 435–464
*http://www.raa-journal.org* *http://www.iop.org/journals/raa*

***R**esearch in*
***A**stronomy and*
***A**strophysics*

# Quark-novae in neutron star - white dwarf binaries: a model for luminous (spin-down powered) sub-Chandrasekhar-mass Type Ia supernovae?

Rachid Ouyed[1] and Jan Staff[2]

[1] Department of Physics and Astronomy, University of Calgary, 2500 University Drive NW, Calgary, Alberta, T2N 1N4 Canada; *rouyed@ucalgary.ca*
[2] Department of Physics and Astronomy, Louisiana State University, 202 Nicholson Hall, Tower Dr., Baton Rouge, LA 70803-4001, USA

Received 2012 September 12; accepted 2012 November 13

**Abstract** We show that, by appealing to a Quark-Nova (QN) in a tight binary system containing a massive neutron star and a CO white dwarf (WD), a Type Ia explosion could occur. The QN ejecta collides with the WD, driving a shock that triggers carbon burning under degenerate conditions (the QN-Ia). The conditions in the compressed low-mass WD ($M_{\rm WD} < 0.9\,M_{\odot}$) in our model mimic those of a Chandrasekhar mass WD. The spin-down luminosity from the QN compact remnant (the quark star) provides additional power that makes the QN-Ia light-curve brighter and broader than a standard SN-Ia with similar $^{56}$Ni yield. In QNe-Ia, photometry and spectroscopy are not necessarily linked since the kinetic energy of the ejecta has a contribution from spin-down power and nuclear decay. Although QNe-Ia may not obey the Phillips relationship, their brightness and their relatively "normal looking" light-curves mean they could be included in the cosmological sample. Light-curve fitters would be confused by the discrepancy between spectroscopy at peak and photometry and would correct for it by effectively brightening or dimming the QNe-Ia apparent magnitudes, thus over- or under-estimating the true magnitude of these spin-down powered SNe-Ia. Contamination of QNe-Ia in samples of SNe-Ia used for cosmological analyses could systematically bias measurements of cosmological parameters if QNe-Ia are numerous enough at high-redshift. The strong mixing induced by spin-down wind combined with the low $^{56}$Ni yields in QNe-Ia means that these would lack a secondary maximum in the $i$-band despite their luminous nature. We discuss possible QNe-Ia progenitors.

**Key words:** stars: evolution — stars: binary — stars: neutron — stars: white dwarfs — supernovae: general

## 1 INTRODUCTION

Despite their astrophysical significance, as a major contributor to cosmic nucleosynthesis and as distance indicators in observational cosmology, Type Ia supernovae (SNe-Ia) lack theoretical understanding. The evolution leading to explosion and its mechanisms are among the unknowns. The consensus is that SNe-Ia result from thermonuclear explosions of carbon-oxygen (CO) white dwarfs

(WDs; Hoyle & Fowler 1960; Arnett 1982). The explosion proper is generally thought to be triggered when the WD approaches (for accretion) or exceeds (for a merger) the Chandrasekhar mass, and the density and temperature become high enough to start runaway carbon fusion. Detonation models have been proposed for C-burning in the WD interior (Arnett 1969; Nomoto 1982) as well as deflagration models (Woosley & Weaver 1986). A delayed detonation transition (Khokhlov 1991a) may be needed to better replicate observations.

The nature of the progenitors of SNe-Ia is debated. Explosion models of SNe-Ia currently discussed in the literature include explosions of Chandrasekhar mass WDs and their variants (Khokhlov 1991b; Gamezo et al. 2005; Livne et al. 2005; Röpke & Niemeyer 2007; Jackson et al. 2010; Plewa 2007; Jordan et al. 2008; Meakin et al. 2009; Bravo et al. 2009 to cite only a few), explosions of super-massive WDs (e.g. Pfannes et al. 2010 and references therein), and of sub-Chandrasekhar WDs (Woosley et al. 1980; Nomoto 1982; Livne & Glasner 1991; Livne & Arnett 1995; Fink et al. 2010).

In the single degenerate (SD) scenario, if mass transfer is too slow, novae occur, which appear to remove as much mass as was accreted (Townsley & Bildsten 2004). If it is faster, H burns stably, but only a small range of accretion rate avoids expansion and mass-loss (Nomoto et al. 2007). The lack of H in spectra of SNe-Ia is often seen as troublesome for SD progenitor models. On the other hand, in the double-degenerate (DD) scenario, mergers of WDs could give rise to SNe-Ia (Webbink 1984; Iben & Tutukov 1984) and could naturally explain the lack of H. Both SD and DD scenarios may allow super-Chandrasekhar SNe-Ia. If the WD is spun up by accretion to very fast differential rotation (with mean angular velocity of order a few radians per second on average), then the WD may exceed the physical Chandrasekhar mass by up to some tenths of a solar mass before reaching explosive conditions in the central region (Yoon & Langer 2005). Merger simulations did not result in an explosion (e.g. Saio & Nomoto 2004), but rather they indicate that an off-center ignition causes the C and O to be converted to O, Ne, and Mg, generating a gravitational collapse rather than a thermonuclear disruption (Nomoto & Iben 1985). This is the so-called accretion-induced collapse (AIC) to an NS where C is not ignited explosively but quietly, yielding a faint explosion and an NS remnant instead of an SN-Ia (see also Stritzinger & Leibundgut 2005).

### 1.1 Sub-Chandrasekhar Mass Models

Theoretical and numerical (hydrodynamical) studies have previously shown that sub-Chandrasekhar mass WDs with an overlying helium shell (accreted from a companion) can undergo a double-detonation which could lead to an SN-Ia (Woosley et al. 1980; Nomoto 1982; Livne & Glasner 1990; Livne & Glasner 1991; Livne & Arnett 1995; Fink et al. 2007; Fink et al. 2010). In these models a layer of accreted helium ($\sim 0.1 - 0.2\ M_{\odot}$) is built either by burning accreted hydrogen to helium or by accretion of helium from a helium-rich donor (Woosley & Weaver 1986; Woosley & Weaver 1994; Ivanova & Taam 2004). When the pressure at the base of the helium layer reaches a critical threshold, it detonates, driving a shock into the core of the WD. This causes a second detonation, resulting in a flame propagating outward from the core (or near it), destroying the WD. In edge-lit models, the mass of the WD must increase during the pre-supernova evolution to $\sim 0.9 - 1.1\ M_{\odot}$ to explain typical SN-Ia luminosities (e.g. Woosley & Kasen 2011). This strong constraint on the WD mass is due to the fact that core densities $> 2.5 \times 10^7$ g cm$^{-3}$ are required for the detonation to produce enough radioactive nickel (Sim et al. 2010) and to survive nova-like outbursts at the high accretion rate which actually shrink the WD mass. Specifically, the WD mass should be at least 0.9 $M_{\odot}$ at the time of the SN-Ia (to produce an amount of $^{56}$Ni within the range of normal SNe).

Although physically realistic, the double-detonation sub-Chandrasekhar model may suffer from the fact that even with a very low mass helium layer ($\sim 0.05\ M_{\odot}$) their spectroscopic signatures are not characteristic of observed SNe-Ia (Kromer et al. 2010; see also Ruiter et al. 2011). However, it has recently been argued that the model might be capable of producing a better match to observa-

tions, depending on details regarding the manner in which the accreted helium burns (e.g. Fink et al. 2010). It has also been suggested that a more complex composition of the helium layer may lead to a better agreement with observations but this remains to be confirmed. More recent 1-dimensional simulations show that only the hottest (i.e., with initial luminosity of $\sim L_{\odot}$), most massive WDs considered with the smallest helium layers, show reasonable agreement with the light-curves and spectra of common SNe-Ia (Woosley & Kasen 2011).

In the DD scenario, the less massive WD may be disrupted into a disk from which the more massive WD accretes at a constant rate near the gravitational Eddington limit. Others find that the less massive WD is transformed into a hot, slowly rotating, and radially extended envelope supported by thermal pressure (e.g. Shen et al. 2012 and references therein). It was found that the long-term evolution of the merger remnant is similar to that seen in previous calculations; i.e. an off-center burning eventually yielding a high-mass O/Ne WD or a collapse to an NS, rather than an SNe-Ia (see also Dan et al. 2011). On the other hand, van Kerkwijk et al. (2010) consider the viscous evolution of mergers of equal mass WDs in which both WDs are tidally disrupted (see also Yoon et al. 2007; Lorén-Aguilar et al. 2009; Pakmor et al. 2011). The resulting remnant has a temperature profile that peaks at the center (and is fully mixed), unlike remnants in which only one WD is disrupted, which have a temperature peak in material at the edge of the degenerate core.

The sub-Chandrasekhar mass WD mergers (van Kerkwijk et al. 2010) lead to a cold remnant ($\sim 6 \times 10^8$ K) with central densities $\sim 2.5 \times 10^6$ g cm$^{-3}$. However, accretion of the thick "disk" leads to compressional heating resulting in an increase in the central temperature to $\sim 10^9$ K and densities $\sim 1.6 \times 10^7$ g cm$^{-3}$. These conditions, they argue, could ignite the center region of the remnant with the nuclear runaway as an inevitable result. In this scenario, van Kerkwijk et al. (2010) argued that SNe-Ia result from mergers of CO WDs, even those with sub-Chandrasekhar total mass. Badenes & Maoz (2012) find a remarkable agreement between the total WD merger rate and the SN-Ia rate, but not enough close binary WD systems to reproduce the observed Type Ia SN rate in the classic DD scenario. Apart from the consistency between SN-Ia rates and total WD merger rates, sub-Chandrasekhar explosions may have the advantage of producing the correct chemical stratification (Sim et al. 2010), without resorting to the delayed detonation mechanism (Khokhlov 1991a) needed by super-Chandrasekhar models. We note that these simulations begin with the binary components close enough that strong mass transfer immediately sets in once the calculation is begun. By contrast, Dan et al. (2011) emphasize the importance of beginning such simulations at larger orbital separations and instead find tidal disruption at a much larger radius with correspondingly less violence.

We would like to mention other alternative progenitor scenarios to produce SNe-Ia explosions, which are not restricted to the ignition of a CO WD near the Chandrasekhar mass. One scenario involves tidal disruption of white dwarfs by moderately massive black holes (Rosswog et al. 2009a) and another involves a shock-triggered thermonuclear explosion from the collision of two WDs (Rosswog et al. 2009b). See also Milgrom & Usov (2000) for descriptions of Type Ia explosions triggered by gamma-ray bursts. For a detailed discussion on the open issue of SN-Ia progenitors, we refer the interested reader to several reviews (e.g., Branch et al. 1995; Renzini 1996; Livio 2000). Overall, the models described above, and those listed in the reviews above, differ in their assumptions about initial conditions, ignition processes, whether the explosion involves subsonic deflagration or not, and other details, and they have varying success in explaining basic observations of SNe-Ia. A common feature of the models is that all of them involve, in one way or another, the detonation mode of burning. However, the lack of convincing solutions to the progenitor(s) of SNe-Ia leaves room for an alternative. Here we present a new channel for Type Ias (SNe-Ia) by appealing to a Quark-Nova explosion (hereafter QN; Ouyed et al. 2002; Keränen et al. 2005) in a close NS-WD (CO) binary system. Under appropriate conditions, C-burning is triggered by shock compression and heating from the relativistic QN ejecta (QNE) impacting the WD leading to a Type Ia explosion. Hereafter, we refer to these QN-triggered type Ias as QNe-Ia.

The basic picture of the QN is that a massive NS converts explosively to a quark star (Ouyed et al. 2002; Keränen et al. 2005). Such an explosion can happen if the NS reaches the quark deconfinement density via spin-down or accretion (Staff et al. 2006) and subsequently undergoes a phase transition to the conjectured more stable strange quark matter phase (Itoh 1970; Bodmer 1971; Witten 1984; see also Terazawa 1979), resulting in a conversion front that propagates toward the surface in the detonative regime (Niebergal et al. 2010) – *a hypothesis* we adopt in this paper (as in previous work) based on preliminary 1D simulations. The outcome is ejection of the NS's outermost layers at relativistic speeds. The outer layers are ejected from an expanding thermal fireball (Vogt et al. 2004; Ouyed et al. 2005) which allows for ejecta with kinetic energy, $E_{\rm QN}^{\rm KE}$, in the $10^{52}$ erg range. In previous papers, we introduced the QN as a model for superluminous SNe (Leahy & Ouyed 2008; Ouyed & Leahy 2012), discussed their photometric/spectroscopic signatures (Ouyed et al. 2012) as well as their nuclear/spallation signatures from the interaction of the ultra-relativistic neutrons with the preceding SN shells and surroundings (Ouyed et al. 2011c; see also Ouyed 2012). We also explored conditions for QNe to occur in binaries with applications to gamma-ray bursts (GRBs) (Ouyed et al. 2011a,b).

Here we present a model in the context of QNe occurring in NS-WD systems and show how luminous sub-Chandrasekhar mass Ia explosions could in principle occur. This paper bears similarities to those of Ouyed et al. (2011b), but considers more carefully both the interaction between the QNE and the WD and considers the implication of the spin-down luminosity of the QN compact remnant (the quark star) on the resulting light-curve. In Ouyed et al. (2011b) we explored both the relativistic and non-relativistic degenerate regime while here we focus solely on the relativistic regime and consider only $M_{\rm WD} >\sim 0.5\ M_\odot$. The main differences between QNe-Ia and standard SNe-Ia are: (i) A QN-Ia involves the detonation of a sub-Chandrasekhar mass WD ($M_{\rm WD} < 0.9\, M_\odot$) in a close NS-WD (CO) binary system with orbital separation $< 10^{10}$ cm. This hints at specific progenitors as discussed in this paper; (ii) Burning in QNe-Ia occurs following impact by the relativistic QNE. The compression and heating of the WD mimic burning conditions (densities and temperature) reminiscent of those in Chandrasekhar mass models although the CO WD in our model is truly in a sub-Chandrasekhar mass regime; (iii) In addition to $^{56}$Ni decay, spin-down power from the QN compact remnant (the quark star) provides an additional energy source that powers the explosion. This additional energy source is unique to our model and has the potential of altering the shape (i.e. morphology) of the light-curve. Readers who wish to understand the essential differences and/or differentiating predictions of our model compared to standard SNe-Ia are referred to Section 3.

The paper is organized as follows: In Section 2, we give a brief description of the QN. In Section 3 we describe the collision between the QNE and the WD and explore conditions for C-detonation to occur in NS-WD systems experiencing a QN. In this section, we explain how the QN can lead to a thermonuclear runaway in the companion WD. Here, we discuss the resulting nuclear products. The spectrum and the light-curve are discussed in Section 4. In particular, we investigate how spin-down luminosity alters the resulting light-curve and discuss plausible QNe-Ia candidates among peculiar SNe-Ia. In Section 5 we present possible QNe-Ia progenitors and their occurrence rates. In Section 6 we discuss a plausible QN-Ia connection to massive star formation and its implications to cosmology and dark energy. Specific predictions and a conclusion are given in Section 7.

## 2 THE QUARK-NOVA

### 2.1 The Exploding Neutron Star

As in Staff et al. (2006), we assume the deconfinement density of $\rho_{\rm c} = 5\rho_{\rm N} \simeq 1.25 \times 10^{15}$ g cm$^{-3}$ where $\rho_{\rm N} = 2.85 \times 10^{14}$ g cm$^{-3}$ is the nuclear saturation density. For the APR equation of state (EoS) (Akmal et al. 1998), which we adopt in this paper, a static configuration (i.e. non-rotating NS) of $M_{\rm NS,c} \sim 1.8\, M_\odot$ reaches $\rho = \rho_{\rm c}$ in its core, thus being prone to the QN explosion. Stiffer EoSs (e.g. Ouyed & Butler 1999) extend the critical NS mass to higher values ($M_{\rm NS,c}\sim\ 2\, M_\odot$) while

softer EoSs (e.g. BBB2; Baldo et al. 1997) give lower values ($M_{\rm NS,c} \sim 1.6\,M_\odot$). We note that all of these EoSs allow for NSs with maximum masses higher than the $M_{\rm NS,c}$. The QN effectively reduces the maximum mass allowed by a given EoS to $M_{\rm NS,c}$. Naturally, rapidly rotating configurations will increase the mass limit.

There are two possible paths to reaching deconfinement in the core of an NS:

(i) Via spin-down if the NS is born with a mass above $M_{\rm NS,c}$ but fully recycled ($< 2$ ms); the fast rotation decreases the core density below the $\rho_{\rm c} = 5\rho_{\rm N}$ limit. Staff et al. (2006) considered the parameter-space in mass, magnetic field and spin-period to identify how long such an NS would take to reach the quark deconfinement density. They found that NSs with mass $> M_{\rm NS,c}$, spin period $\sim 2$ ms and magnetic field $\sim 10^9$ G ($10^8$ G) will reach deconfinement density in $\tau_{\rm QN} < 10^8$ ($10^{10}$) yr due to the spin-down effect from dipole radiation, leading to an increase in the star's central density to the quark deconfinement limit.

(ii) If the NS is born massive enough (very close to the critical NS mass $M_{\rm NS,c}$) and mildly or slowly rotating; In this case, a slight increase in its mass by accretion will push its core density above the deconfinement value which triggers the explosive instability. The combined effect of increase in the core density from the added mass and its decrease from NS spin-up leads to an overall increase of a few percent in the NS core density. This scenario requires the NS mass (core density) to be within a few percent or $M_{\rm NS,c}$ (or $\rho_{\rm c}$) to explode as a QN when it accretes.

The mass limit, $M_{\rm NS,c}$, set by the QN means that NSs heavier than $M_{\rm NS,c}$ should not exist (if QNe were to occur) in nature in contradiction with the recent observations of a $2\,M_\odot$ NS (Demorest et al. 2010). However, $M_{\rm NS,c}$ could be made to exceed $\sim 2\,M_\odot$ if we set the deconfinement density above $5\rho_{\rm N}$ as is the case for the APR EoS whose maximum gravitational mass exceeds $2\,M_\odot$. It is also possible that NSs more massive than $M_{\rm NS,c}$ are really quark or hybrid stars (that is, the quark matter EoS should be sufficiently stiff to support such a mass)[1]. Heavy quark stars may exist, so long as the quark superconducting gap and strong coupling corrections are taken into account (Alford et al. 2007). The BBB2 EoS is too soft and provides a maximum gravitational mass of $\sim 1.9\,M_\odot$ but if the observed massive NS is really a quark or hybrid star, we cannot rule out BBB2 in this way, and its inclusion is still useful.

### 2.2 The QN Compact Remnant: the Quark Star

In the QN model, we assume that hot quark matter in the Color-Flavor-Locked (CFL) phase is the true ground state of matter at high density (Alford et al. 1999). This is a superconducting phase that is energetically favored at extremely high densities and low temperatures. In this phase u, d, and s quarks pair, forming a quark condensate (a superfluid) that is antisymmetric in color and flavor indices. This state is reached by the QN compact remnant (a quark star (QS) in the CFL phase) as it cools below a few tens of MeV. The initial QS surface magnetic field is of the order of $10^{14} - 10^{15}$ G (Iwazaki 2005); we adopt $10^{14}$ G as a fiducial value.

Spin-down of the QN compact remnant due to magnetic braking can naturally lead to the launching of a secondary outflow in the form of a pair wind. The corresponding spin-down (lower case subscript $sd$) luminosity is $L_{\rm sd} \sim 6.4 \times 10^{43}\ {\rm erg\,s^{-1}}\ B^2_{\rm QS,14} P^{-4}_{\rm QS,10} (1 + t/\tau_{\rm sd})^{-5/3}$ where $\tau_{\rm sd} \simeq 100\ {\rm d}\ B^{-2}_{\rm QS,14} P^2_{\rm QS,10}$ (Staff et al. 2008; see Contopoulos & Spitkovsky 2006 for spin-down power for an aligned rotator). Here the QS magnetic field is given in units of $10^{14}$ G and the period in units of 10 ms, i.e. a rotational energy (an additional energy source) of $\sim 2 \times 10^{50} P^{-2}_{\rm QS,10}$ not present in any of the standard (i.e. $^{56}$Ni powered) models of Type Ia SNe; the QS moment of inertia

[1] While it is almost certain that the (u,d,s) phase, if it exists inside NSs, cannot be a free gas of quarks (Özel et al. 2010; Weissenborn et al. 2011), an interacting phase of quarks still appears to be consistent with the recent finding of a $2\,M_\odot$ NS (Demorest et al. 2010).

is set to $2 \times 10^{45}$ g cm$^2$. The implications for QNe-Ia light curves (with plausible deviations from the Phillips relationship) are presented in Section 4.1.

### 2.3 The Quark Nova Ejecta (QNE)

The QN proper (i.e. the explosion) will happen on timescales of milliseconds (Ouyed et al. 2005; Niebergal et al. 2010) ejecting the outermost layers of the parent NS (Keränen et al. 2005) at relativistic speeds with an average Lorentz factor $\Gamma_{\rm QN} \sim 10$. The evolution of the QNE from point of explosion is given in appendix B in Ouyed & Leahy (2009) with the QNE density $\rho_{\rm QNE}$ at a distance $r = a$ from the point of explosion derived from a combination of mass conservation and thermal spreading of the QN ejecta thickness, $\Delta r$. This gives

$$\rho_{\rm QNE} \sim 1.8 \times 10^6 \ {\rm g\ cm^{-3}} \times \frac{\rho_{0,14} \Delta r_{0,4}}{a_9^{9/4} M_{\rm QN,-3}^{1/4}} \ , \qquad (1)$$

where $\rho_0$, the QNE density at explosion radius, is given in units of $10^{14}$ g cm$^{-3}$; for a typical ejecta mass $M_{\rm QNE} \sim 10^{-3}\ M_\odot$. The thickness at ejection is $\Delta r_0 \sim 10^4$ cm or $\Delta r_{0,4} \sim 1$ in units of $10^4$ cm; the distance from the explosion point (later to be defined as the binary separation), $a_9$, is given in units of $10^9$ cm.

### 2.4 Specific Observational Signatures of QNe

While this paper explores observational signatures of QNe going off in binary systems, we briefly mention some specific and unique signatures of QNe going off in isolation. In particular, dual-shock QNe (i.e. QNe going off a few days to a few weeks following the preceding type II SN explosion) offer the most promising observables. The interaction of the QNE with the preceding SN ejecta leads to the re-energization of the SN shell which should manifest itself in the optical as a "double-hump" lightcurve with the first, smaller, hump corresponding to the core-collapse SN proper and the second hump to the re-energized SN ejecta (Ouyed et al. 2009). A strong contender for the double-humped lightcurve is the super-luminous supernova SN 2006oz as reported in Ouyed & Leahy (2012; see also Ouyed et al. 2012).

Besides the re-energization of the preceding ejecta from the Type II explosion, the extremely neutron-rich relativistic QNE leads to spallation of the innermost layers of the SN shell thus destroying $^{56}$Ni while forming sub-Ni elements. One distinguishable feature of this interaction is the production of $^{44}$Ti at the expense of $^{56}$Ni (see Ouyed et al. 2011c) which results in Ni-poor (i.e. subluminous), Ti-rich type II SNe and the proposal of Cas-A as a plausible dual-shock QN candidate (Ouyed et al. 2011c); the QN imprint in Cas A might have been observed (Hwang & Laming 2012). The neutron-rich QN ejecta as it expands away from the NS was shown to make mostly $A > 130$ elements (Jaikumar et al. 2007). We can thus combine photometric and spectroscopic signals that are specific to the QN – and should thus be model-independent – to come up with a plausible, observable candidate. Spectroscopically, the dual-shock QN will exhibit strong $\gamma$-ray signatures from $^{44}$Ti and from $A > 130$ elements. Combining the spectroscopic signal, with the photometric "double hump" of the dual-shock QN light curve, gives a very specific signature of how a QN will appear to observers. In addition, the gravitational wave (GW) signal from the preceding SN and the subsequent QN should be discernible in case of asymmetric explosions (Staff et al. 2012). GW observatories currently in planning may be able to detect these predicted dual-GW signals and may offer some first glimpses of QNe in the near future.

## 3 QN-TRIGGERED CARBON BURNING

Now let us consider a binary system with a massive NS and a CO WD (hereafter MNS-COWD) where the NS experiences a QN episode. We ask at what distance from the NS should the WD

be located when the QN goes off in order to ignite carbon under degenerate conditions? For this purpose, we adopt a WD mass of $0.6\,M_{\odot}$ representative of the empirical mean mass of WDs (e.g. Tremblay & Bergeron 2009; Kepler et al. 2007) with a mean density of $\sim 5\times10^{6}$ g cm$^{-3}$ (e.g. Even & Tohline 2009) – we only consider the relativistic degenerate regime in this paper which puts a lower limit on the WD mass we consider in this work. The WD mass-radius relationship for this regime is (Padmanabhan 2001)

$$\frac{R_{\rm WD}}{R_{\odot}} \simeq \frac{0.011}{\mu_{\rm WD,2}}\left(\frac{M}{M_{\rm Ch}}\right)^{-1/3}\times f(M_{\rm WD})^{1/2}\,, \qquad (2)$$

where $f(M_{\rm WD})=(1-(\frac{M_{\rm WD}}{M_{\rm Ch}})^{4/3})$ and $M_{\rm Ch}=1.435\,M_{\odot}/\mu^{2}_{\rm WD,2}$ the Chandrasekhar limit with $\mu_{\rm WD}$ being the mean molecular weight in units of 2.

### 3.1 The QNE-WD Collision

When the QNE encounters the WD (i.e. a number density jump in $n_{\rm QNE}/n_{\rm WD}$), a reverse shock (RS) is driven into the cold QNE, while a forward shock (FS) propagates into the cold higher density WD material (see Appendix). Therefore, there are four regions separated by the two shocks in this system: (1) unshocked cold WD matter, (2) forward-shocked hot WD matter, (3) reverse-shocked QNE, and (4) unshocked cold QNE. From the shock jump conditions (see Appendix) one can show that the $n_{\rm QNE}/n_{\rm WD}\simeq\Gamma^{2}_{\rm QNE}$ condition separates the Newtonian RS regime ($n_{\rm QNE}/n_{\rm WD}>\Gamma^{2}_{\rm QNE}$) from the relativistic RS regime ($n_{\rm QNE}/n_{\rm WD}<\Gamma^{2}_{\rm QNE}$). When the RS is Newtonian it converts only a very small fraction of the kinetic energy into thermal energy; in this case the Lorentz factor of region 2 (the shocked WD material) relative to the rest frame of the WD (i.e. region 1; also an external observer) is $\Gamma_2\simeq\Gamma_{\rm QNE}$. The relativistic RS limit is the regime where most of the kinetic energy of the QNE is converted to thermal energy by the shocks (in this case $\Gamma_2\simeq(n_{\rm QNE}/n_{\rm WD})^{1/4}\Gamma^{1/2}_{\rm QNE}/\sqrt{2}$). For a recent analytical formulation of relativistic shocks we refer the reader to Uhm (2011; and references therein).

A relativistic RS is the critical condition to substantially heat the QNE. But what matters in our case is the FS, which compresses and heats the WD. After the RS crosses of the QNE, the FS starts to decelerate, so $\Gamma_2$ is a decreasing function of time and radius. More importantly, if by the time the FS has decelerated (i.e. reaches the non-relativistic regime) it has travelled deep enough inside the WD then this raises the possibility of detonating the WD with the FS. The time it takes the RS to cross the QNE (shell) is $\tau_{\rm cros}\simeq\Delta R_{\rm QNE}\Gamma_{\rm QNE}(n_{\rm QNE}/n_{\rm WD})^{1/2}/c$ (e.g. Sari & Piran 1995); $c$ is the speed of light. To first order, since the QNE has a thickness of $\sim100-1000$ km at a distance of $\sim10^{9}-10^{10}$ cm from the explosion (see appendix B in Ouyed & Leahy 2009) and taking $n_{\rm QNE}/n_{\rm WD}\sim\Gamma_{\rm QNE}$, we get $\tau_{\rm cros}\sim0.17$ s $\times\,\Delta R_{\rm QNE,500}\Gamma^{2}_{\rm QNE,10}$; $\Delta R_{\rm QNE,500}$ is in units of 500 km. Thus, the RS lasts for a short period of time. During this time the FS would have reached depths of at least the order of $\Delta R_{\rm QNE}$ (since $\Gamma_{\rm FS}\simeq2\Gamma_{\rm RS}$), i.e. depths of the order of a few thousand kilometers could be reached by the FS under appropriate conditions. We can define a corresponding critical WD density as (combining Eq. (1) and $n_{\rm QNE}/n_{\rm WD}\simeq\Gamma^{2}_{\rm QNE}$)

$$\rho_{\rm WD,c}\sim2\times10^{5}\ {\rm g\ cm^{-3}}\ \times\frac{\rho_{0,14}\Delta r_{0,4}}{\Gamma^{2}_{\rm QNE,10}a_{9}^{9/4}M^{1/4}_{\rm QN,-3}}\,, \qquad (3)$$

where the QNE Lorentz factor is in units of 10. To convert from number density to mass density, we take $\mu_{\rm WD}\sim14$ and $\mu_{\rm QNE}\sim1$ as the mean molecular weight for the WD and QNE, respectively (the QNE remains dominated by neutrons even after the end of the r-process; Jaikumar et al. 2007). The equation above is relevant if the radius at which the density reaches the critical value is smaller than the deceleration radius (which is the RS crossing radius). In general, and to a first approximation,

we arrive at similar results by assuming that the non-relativistic stage would be reached by the FS when the initial energy of the QNE equals roughly the rest mass energy of the WD being shocked. Our treatment of the propagation of the FS shock is very simplified and whether it can propagate that deep in the WD remains to be confirmed by detailed numerical simulations of the QNE-WD interaction. To carry on with our investigation, we assume that for some of our QNE the RS becomes non-relativistic deep inside the WD. Under the right conditions heating and compression could lead to carbon ignition close to the core (i.e. at $R_{\rm WD} < R_{\rm WD,c}$).

We note that the WD is always substantially heated regardless of whether the RS is relativistic or Newtonian. The energy gained by the WD is an important portion of the QN kinetic energy, $E_{\rm WD,th} \sim E^{\rm KE}_{\rm QN} \times \Omega_{\rm WD}$, where $\Omega_{\rm WD} = R^2_{\rm WD}/(4a^2)$ is the solid angle subtended by the WD. Or,

$$E_{\rm WD,th} \sim 4.7 \times 10^{48}\ {\rm erg}\ \frac{\zeta_{\rm QN} E^{\rm KE}_{\rm QN,52}}{a^2_{10}} \frac{f(M_{\rm WD})/0.68}{\mu^{10/3}_{\rm WD,2} M^{2/3}_{\rm WD,0.6}}\ , \tag{4}$$

where we made use of the generalized mass-radius relation for WDs described earlier with $f(0.6\,M_\odot) \sim 0.68$. The factor $\zeta_{\rm QN} < 1$ is relevant to cases where the thermal energy gained by the WD from heating by the QN shock is less than 100%; since lower values of $\zeta_{\rm QN}$ are easily compensated by higher $E^{\rm KE}_{\rm QN}$ values, hereafter we take $\zeta_{\rm QN} = 1$. If (see Sect. 3.2 below) compression and thermalization of the WD occur before ignition, and burning takes place efficiently, then the average temperature per nucleon of the shocked and thermalized WD is

$$T_{\rm SWD} \sim 9.5 \times 10^9\ {\rm K}\ \frac{E^{\rm KE}_{\rm QN,52}}{a^2_9} \frac{f(M_{\rm WD})/0.68}{\mu^{7/3}_{\rm WD,2} M^{5/3}_{\rm WD,0.6}}\ . \tag{5}$$

### 3.2 Shock Compression and Carbon Ignition/Burning

For $\Gamma_{\rm QNE} \gg 1$ the density in the shocked WD material is (see Appendix)

$$\frac{\rho'_{\rm SWD}}{\rho_{\rm WD}} \simeq \Gamma_2 \times (4\Gamma_2 + 3)\ , \tag{6}$$

or $\rho'_{\rm SWD}/\rho_{\rm WD} \propto \Gamma^2_2$, where $\rho'_{\rm SWD}$ is the density of the shocked WD material in the WD (i.e. observer's) frame. We note that even for a non-relativistic RS, $\Gamma_2$ can be as high, or even higher than, $\Gamma_{\rm QNE}$ (e.g. Zhang & Kobayashi 2005).

In principle, the WD compression ratio can reach values of tens or hundreds. For our fiducial values, the above translates to (order of magnitude estimates of the compression ratio of)

$$\frac{\rho'_{\rm SWD}}{\rho_{\rm WD}} \sim \begin{cases} 430 & \text{if } \rho_{\rm WD} \le \rho_{\rm WD,c} \text{ since } \Gamma_2 = \Gamma_{\rm QNE} \\ < 217 & \text{if } \rho_{\rm WD} > \rho_{\rm WD,c} \text{ since } \Gamma_2 < 2.3\Gamma_{\rm QNE}. \end{cases} \tag{7}$$

In general then it is not unrealistic to assume that solutions can be found where the shocked WD might be compressed to average densities of $\sim 10^8$ g cm$^{-3}$ in its core and average densities of $\sim 10^7$ g cm$^{-3}$ in its surface layers. While the highest compression will most likely be achieved in the WD surface layers, these will most likely experience minimal heating. Thus, ignition and burning (if they occur successfully), we speculate, will most likely be triggered in regions deeper than $R_{\rm WD,c}$ where higher temperatures are reached.

Correctly modeling the process that leads to successful ignition in our model requires a more elaborate treatment (i.e. detailed numerical simulations) of the shock including necessary physics such as neutrino losses, diffusive processes, turbulence and so forth (e.g. Dursi & Timmes 2006). Here we can only provide very qualitative arguments that allow us to speculate that a suitable shock (i.e. with a relativistic FS travelling deep inside the WD) could in principle ignite the

WD successfully: the nuclear burning timescale (Woosley et al. 2004) behind the shock in our case can be estimated to be $\tau_{\rm nuc} \sim 1.153 \times 10^{-20}$ s $(10^{10}$ K$/T_{\rm SWD})^{22}(10^8$ g cm$^{-3}/\rho_{\rm SWD})^{3.3}$. The timescale on which the WD can react, its dynamical timescale, is $\tau_{\rm dyn}= (G\rho_{\rm WD})^{-1/2} \sim 1.7$ s $(5 \times 10^6$ g cm$^{-3}/\rho_{\rm WD})^{1/2}$. Only in scenarios where $\tau_{\rm dyn}$ is much shorter than the burning timescale $\tau_{\rm nuc}$ would the WD respond fast enough to quench burning by a reduction of density and temperature. Appreciable burning will take place if $\tau_{\rm nuc} < \tau_{\rm dyn}$ or if $T_{\rm SWD} > 10^9$ K $\times$ $(\rho_{\rm SWD}/10^8$ g cm$^{-3})^{-2.8/22}$. Combined with Equation (5) this gives

$$a_9 < a_{\rm nuc,9} \sim 3.1 \times (E^{\rm KE}_{\rm QN,52})^{1/2} \frac{(f(M_{\rm WD})/0.68)^{1/2}}{\mu^{7/6}_{\rm WD,2} M^{5/6}_{\rm WD,0.6} \rho^{-2.8/44}_{\rm SWD,8}} \, , \tag{8}$$

where the shocked WD density $\rho_{\rm SWD,8}$ is in units of $10^8$ g cm$^{-3}$. Note the very weak dependence of $a_{\rm nuc,9}$ on $\rho_{\rm SWD}$. To continue with our investigation we assume that the condition $\tau_{\rm cros} < \tau_{\rm nuc} < \tau_{\rm dyn}$ is met, i.e., the ignition and burning timescales are to first order shorter than the dynamical timescale.

The constraint above also guarantees that the average temperature of the shocked WD is high enough to burn carbon ($T_{\rm SWD} > T_{\rm C} \simeq 7 \times 10^8$ K; e.g. Nomoto 1982). The $T_{\rm SWD} > T_{\rm C}$ condition puts a constraint on the separation between the MNS and the COWD

$$a_9 < a_{\rm C,9} \simeq 3.7 \times (E^{\rm KE}_{\rm QN,52})^{1/2} \frac{(f(M_{\rm WD})/0.68)^{1/2}}{\mu^{7/6}_{\rm WD,2} M^{5/6}_{\rm WD,0.6}} \, , \tag{9}$$

which shows that $a_{\rm C} > a_{\rm nuc}$ can be safely assumed given the weak dependence of $a_{\rm nu}$ on $\rho_{\rm SWD}$. This allows the effective collapse of Equations (8) and (9) to one equation with $T_{\rm C}$ as the free common parameter. Hereafter we restrict ourselves to $a < a_{\rm C,10}$. Furthermore, burning occurs under degenerate conditions since the Fermi temperature for the WD relativistic gas (e.g. Shapiro & Teukolsky 1983; p24), $T_{\rm F} \sim 2 \times 10^{10}$ K $\times$ $(\rho/10^8$ g cm$^{-3})^{1/3}$, guarantees $T_{\rm F} > T_{\rm SWD} > T_{\rm C}$ in our model. The $T_{\rm F} > T_{\rm SWD}$ puts a lower limit on the WD mass in the helium WD regime which we do not consider here.

The constraint on the binary separation $a < a_{\rm C}$ hints at tight MNS-COWD systems. The tightest orbit is reached when the WD overflows its Roche lobe (RL) at

$$a = a_{\rm RL} \simeq 2.2 \times 10^9 \, {\rm cm} \times \frac{g(q)}{M^{1/3}_{\rm WD,0.6}} \, , \tag{10}$$

where $g(q) = 0.6 + q^{-2/3} \ln(1 + q^{1/3})$ (Eggleton 1983).

Figure 1 shows the range in WD mass which satisfies $a_{\rm RL} \leq a < a_{\rm C}$ when the QN goes off. The range is $0.5\,M_\odot < M_{\rm WD} < 0.9\,M_\odot$ for our fiducial values. The lower limit as we have said is because we only consider CO WDs in a relativistic degenerate regime. The upper limit $\sim 0.9\,M_\odot$, is restricted by the maximum $E^{\rm KE}_{\rm QN}$ value adopted. We note that for high $T_{\rm C}$ values, solutions are found by increasing the kinetic energy of the QN ejecta. In Figure 1, the $M_{\rm NS,c} = 1.6\,M_\odot$ lower NS mass limit corresponds to the BBB2 EoS which is the softest EoS we adopted in our calculations. The $M_{\rm NS,c}= 1.8\,M_\odot$ corresponds to the APR EoS. The vertical dashed line shows the $q = 0.5$ limit which we assume defines the non-merging (i.e. $q \leq 0.5$) regime.

The WD mass range in our model implies $q = M_{\rm WD}/M_{\rm NS} \leq 0.5$ (see Fig. 1) which means that the binary system may not merge. Instead when the orbital separation shrinks below $a_{\rm RL}$, accretion from the WD onto the NS ensues which then increases orbital separation above $a_{\rm RL}$. The system eventually stabilizes itself around $a_{\rm RL}$ (e.g. D'Souza et al. 2006) within the optimum orbital separation ($a_{\rm RL} < a < a_{\rm C}$) for the WD to explode as a Type Ia when it is impacted by the QN shock[2].

[2] The case where the QN goes off when $a < a_{\rm RL}$ requires a separate treatment (and will be explored elsewhere) since one needs to take into account the WD radius increase following the RL overflow and possible temporary lifting of degeneracy.

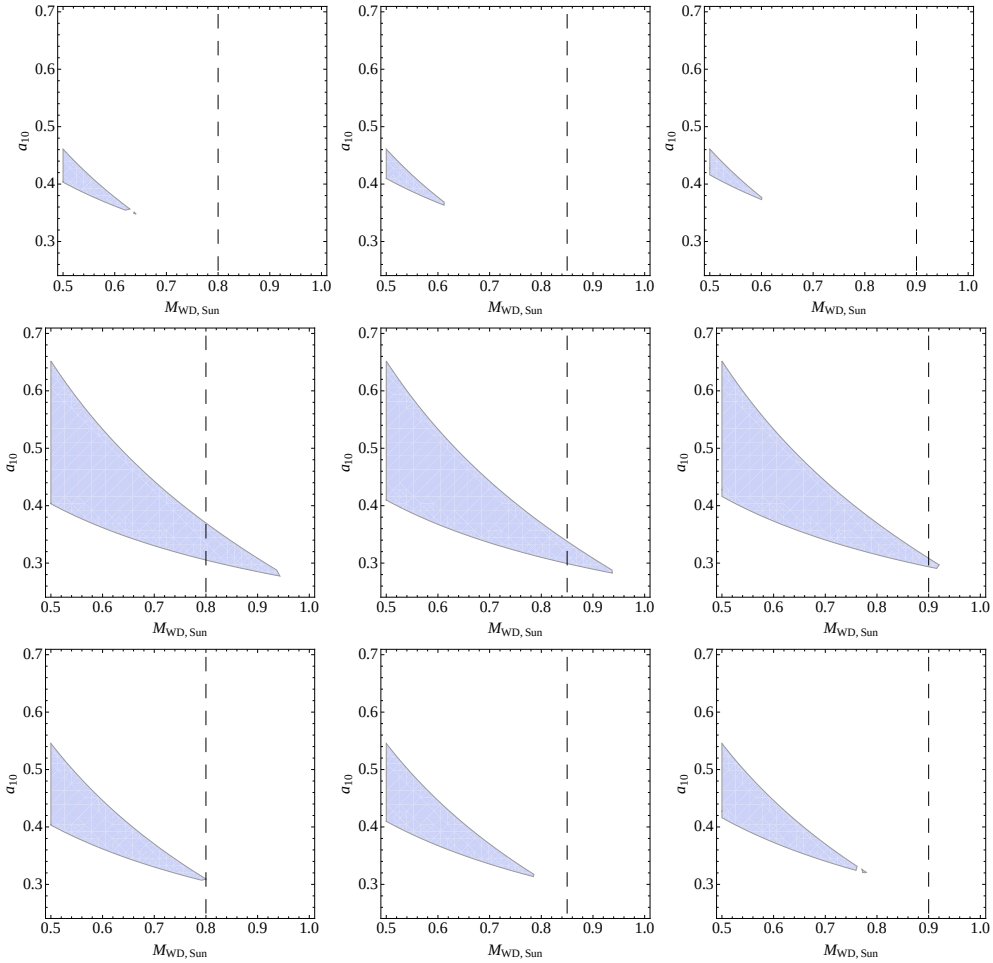


**Fig. 1** The range in WD mass and orbital separation (in units of $10^{10}$ cm) that could result in runaway C-burning after QN impact for $M_{\rm NS} = 1.6\,M_\odot, 1.7\,M_\odot$ and $1.8\,M_\odot$ from left to right, respectively. *Top panels*: $T_{\rm C} = 7 \times 10^8$ K and $E^{\rm KE}_{\rm QN,52} = 1.0$. *Middle panels*: $T_{\rm C} = 7 \times 10^8$ K and $E^{\rm KE}_{\rm QN,52} = 2.0$. *Bottom panels*: $T_{\rm C} = 10^9$ K and $E^{\rm KE}_{\rm QN,52} = 2.0$. Higher $T_{\rm C}$ requires slightly higher $E^{\rm KE}_{\rm QN}$.

Recall that the NS would have been born very close to $M_{\rm NS,c}$ (see Sect. 2.1), such that very little accretion can cause a QN (i.e. before much angular momentum has been accreted). It is ideal then for the NS to explode when the system has settled into an $a \sim a_{\rm RL}$ configuration which points at specific QN-Ia progenitors as discussed in Section 5.

Our model is fundamentally different from other sub-Chandrasekhar models since the extreme compression by the QN shock creates conditions close to higher mass WDs with average densities exceeding $\sim 10^8$ g cm$^{-3}$ (see discussion in Sect. 5.1). It remains to be proven that the high densities and temperatures can successfully ignite carbon which would require extensive numerical simulations to answer. These would include the details of shock compression, propagation and subsequent ignition. For now, we would argue that our model possesses features that could lead to homogenous and efficient ignition in the core (or perhaps near the $\sim R_{\rm WD,c}$ region) of the shocked WD configuration.

### 3.3 Nuclear Products

A distinctive feature of SNe-Ia spectra near maximum light is the presence of intermediate-mass elements (IMEs) from Si to Ca, moving at velocities of 10 000 to 16 000 km $s^{-1}$ (Pskovskii 1969; Branch et al. 1982, 1983; Khokhlov 1989; Gamezo et al. 1999; Sharpe 1999). According to observations, $\sim 0.2 - 0.4\ M_\odot$ of IMEs have to be synthesized during the explosion (see also Iwamoto et al. 1999). Here we discuss the production of Iron-Peak Elements (IPEs) and IMEs in our model while the resulting expansion velocities are discussed in Section 4.

IPEs are produced in regions that reach $\sim 4 \times 10^9$ K before degeneracy is lifted, which requires a density $\rho \geq 10^7$ g $cm^{-3}$ (and $\rho \geq 2 \times 10^6$ g $cm^{-3}$ for IMEs; e.g. Woosley & Weaver 1986). For the same reason, ignition in single-degenerate sub-Chandrasekhar mass WD models requires $M_{\rm WD} > 0.9\,M_\odot$; for lower WD mass the $^{56}$Ni yield is tiny (Sim et al. 2010). As noted earlier, the sub-Chandrasekhar mass WD mergers (van Kerkwijk et al. 2010) lead to a cold remnant ($\sim 6 \times 10^8$ K) with central densities $\sim 2.5 \times 10^6$ g $cm^{-3}$. However, accretion of the thick "disk" leads to compressional heating resulting in an increase in the central temperature to $\sim 10^9$ K and densities $\sim 1.6 \times 10^7$ g $cm^{-3}$. These conditions they argue could ignite the remnant centrally with the nuclear runaway being inevitable. These centrally detonated WDs look like ordinary SNe-Ia (Sim et al. 2010; Kromer et al. 2010) and remove the need for a deflagration; meaning that a deflagration is not necessary to produce the observed IMEs.

While compression and heating in the van Kerkwijk et al. (2010) case is provided by accretion, in our model it is provided by the QNE impact. If ignition occurs in (or close to) the center as we argued in Section 3.2, then in principle the resulting explosion should produce a composition relatively similar to what is observed. However, the very small WD mass in our model ($M_{\rm WD} < 0.9\,M_\odot$) and the extreme compressions from the QN shock could mean that more IPEs are produced at the expense of IMEs.

It is hard to estimate the exact amount of IMEs produced in QNe-Ia explosions without detailed simulations but an order of magnitude estimate is arrived at as follows: For our fiducial values, we estimate that only a small percentage ($< 10\%$) of the WD radius (or rather at most a few percent of the WD mass) encloses densities less than $10^5$–$10^6$ g $cm^{-3}$ (e.g. Even & Tohline 2009). The shock will compress these layers to an average density of $\sim 10^7$ g $cm^{-3}$ where IMEs can eventually be produced. Given these rough numbers above, it is not unreasonable to assume that typical QNe-Ia, at least for the fiducial values we chose, could convert up to 90% of the WD mass into $^{56}$Ni (and thus IPEs) and at most 10% into IMEs, i.e. that on average a typical QN-Ia involving the explosion of $\sim 0.6\,M_\odot$ WD would produce, under optimum conditions, up to $\sim 0.45\,M_\odot$ of $^{56}$Ni (i.e. of IPEs). Lower mass CO WDs, with a higher percentage of their mass at densities below $10^6$ g $cm^{-3}$ (Even & Tohline 2009), would be compressed less and should produce more IMEs at the expense of $^{56}$Ni. These numbers should serve as a very rough estimation of the average $^{56}$Ni yields in our model. Quantitative evaluation of the $^{56}$Ni yields awaits detailed simulation. Hereafter we adopt $M_{\rm Ni} \sim 0.3\,M_\odot$ as our fiducial value for the average $^{56}$Ni yield in a typical QN-Ia.

In the standard models of SNe-Ia, the diversity of SNe-Ia reflected in the range of peak luminosity provides a direct measure of the mass of $^{56}$Ni ejected/synthesized, varying from $\sim 0.1\,M_\odot$ associated with the sub-luminous objects to $\sim 1.3\,M_\odot$ for the most luminous events (e.g. Stritzinger et al. 2006a; Wang et al. 2008 to cite only a few). A number of potential parameters could influence the amount of $^{56}$Ni produced, e.g., C-O ratio, overall metallicity, central density, the ignition intensity, the number of ignition points in the center of WDs or the transition density from deflagration to detonation as well as asymmetry in the explosion (e.g. Timmes et al. 2003; Röpke & Hillebrandt 2004; Röpke et al. 2005; Stritzinger et al. 2006b; Lesaffre et al. 2006; Podsiadlowski et al. 2008; Kasen et al. 2009; Höflich et al. 2010; Meng & Yang 2011). Nevertheless, it seems that the origin of the variation of the amount of $^{56}$Ni for different SNe-Ia is still unclear.

Our model might provide a range in $^{56}$Ni mass by a one parameter sequence in terms of the WD mass, if all QNe-Ia were to occur (or be triggered) when $a = a_{\rm RL}$. Other fiducial parameters such as $\Gamma_{\rm QNE}$ do not vary much from one system to another since the condition for QN explosion is a universal one defined by the quark deconfinement density (here chosen to be $5\rho_{\rm N}$). However, the upper COWD mass in our model ($\sim 0.9\,M_{\odot}$) means that to account for the extreme (up to $\sim 1.3\,M_{\odot}$) masses of $^{56}$Ni observed, one might require the SD, the sub-Chandrasekhar WD mergers, and/or DD channel. As we show below, spin-down power from the QS could brighten the explosion mimicking standard SNe-Ia with $M_{\rm Ni} > 1\,M_{\odot}$. In other words, these spin-down powered QNe-Ia could be mis-interpreted as standard SNe-Ia with much higher $^{56}$Ni content than what is truly processed/produced.

## 4 THE LIGHT-CURVE AND THE SPECTRUM

### 4.1 The Bolometric Light-Curve

In standard SNe-Ia, the ejecta remain optically thick for the first several months after explosion. The width of the bolometric light curve is related to the photon diffusion time, $\tau_{\rm d}$. The peak of the light-curve is directly related to the mass of $^{56}$Ni produced by the explosion. If powered by $^{56}$Ni decay alone (hereafter $^{56}$Ni-powered meaning powered by $^{56}$Ni and $^{56}$Co decay), QNe should produce light-curves that most likely obey the Phillips relationship (i.e. in the $B$-band). On average, QNe-Ia should appear less broad and dimmer (with $M_{\rm Ni} < 0.45\,M_{\odot}$; we adopt an average of $M_{\rm Ni} \sim 0.3\,M_{\odot}$) than their Chandrasekhar mass counterparts (with $M_{\rm Ni} \sim 0.6\,M_{\odot}$). However, there are reasons to expect QNe-Ia to be brighter with broader light-curves than standard SNe-Ia of similar $^{56}$Ni yields if a mildly or a rapidly rotating QS is left behind by the QN. The energy deposited into the expanding WD ejecta by the spinning-down QS can substantially brighten the light-curve, or at least it can compete with the decay of $^{56}$Ni and thermal energy in the expanding WD material. This is reminiscent of powering of Type II SNe shells by pulsar spin-down. Maeda et al. (2007) proposed that some ultraluminous supernovae may be explained by dipole emission from a rapidly spinning magnetar, which was worked out in detail by Kasen & Bildsten (2010) and Woosley (2010). In the early stages, the majority of the spin-down energy is lost to adiabatic expansion and not seen directly in the peak luminosity. Eventually, a percentage of the energy goes into kinetic energy of expansion, while the remainder goes into radiation. Depending on the magnetic field strength and the NS's initial period, these studies find that a percentage (up to $\sim 50\%$) of the spin-down energy went into kinetic energy of expansion, while the remainder went into radiation. In certain cases, the spin-down powered ejecta could lead to a light-curve peak of about a few times the peak luminosity of typical SNe-Ia. Furthermore, the resulting light-curves are broader than those without the spin-down power injection.

As in these models, the spin-down energy in QNe-Ia should result in an additional entropy injection (on timescales exceeding the adiabatic expansion phase) that should brighten the light-curve and perhaps modify its shape. The energy can accelerate the WD ejecta to slightly higher "coasting" velocities than in standard (purely $^{56}$Ni-powered) SNe-Ia. The tail of the light-curve could resemble radioactive decay for some time but, assuming complete trapping of the spin-down emission, would eventually be brighter (e.g. Woosley 2010). In other words, compared to light-curves from purely $^{56}$Ni-powered cases, QNe-Ia light-curves should show some differences in the rise and fall time. From these considerations, we are tempted to argue that QNe-Ia light-curves should not obey the Phillips relationship. However, the light-curve in the $B$-band would need to be computed to corroborate this point.

No simple analytic solution for the bolometric light-curve exists when taking into account $^{56}$Ni-decay power and spin-down power. Instead we make use of semi-analytical models presented in Chatzopoulos et al. (2012) to illustrate our point (assuming that the spin-down energy is thermalized throughout the expanding WD material). In the left panel in Figure 2 we compare a standard purely

$^{56}$Ni-powered SN-Ia with $M_{\rm Ni} = 0.3\,M_\odot$ and diffusion time $\tau_{\rm d} = 30\,{\rm d}$ (the dotted line) to a QN-Ia (the dashed line) with $M_{\rm Ni} = 0.3\,M_\odot$ but boosted by spin-down energy of $2 \times 10^{50}$ erg (i.e. $P_{\rm QS} = 10$ ms) and $\tau_{\rm sd} = 4.5\tau_{\rm d}$ (i.e. $B_{\rm QS} \simeq 9 \times 10^{13}$ G); we keep $\zeta_{\rm sd} = 0.5$ (i.e. half of the spin-down energy went into radiation). This illustration, together with what has been inferred from the above mentioned studies, suggests that QNe-Ia should be brighter and broader than their purely $^{56}$Ni-powered counterparts of similar $^{56}$Ni yield. For a comparison we also show a purely $^{56}$Ni-powered SN-Ia with $M_{\rm Ni} = 0.7\,M_\odot$ and $\tau_{\rm d} = 40\,{\rm d}$. It was chosen so that it closely overlaps with the QN-Ia light-curve. It is shown as the solid line in both panels of Figure 2.

To demonstrate the effect of the spin-down timescale on the light-curves, the right panel in Figure 2 compares our chosen standard SN-Ia to a typical QN-Ia (i.e. $M_{\rm Ni} = 0.3\,M_\odot$, $E_{\rm sd} = 2\times10^{50}$ erg and $\zeta_{\rm sd} = 0.5$) but for different $\tau_{\rm sd}$; $\tau_{\rm sd} = 60\,{\rm d}$ (the dashed line) and the other $\tau_{\rm sd} = 3\,{\rm d}$ (the dotted line). While the $\tau_{\rm sd} = 3\,{\rm d}$ QN-Ia is narrower, a slight increase in its $^{56}$Ni content will make it broader and brighter than the standard SN-Ia. We find that although QNe-Ia are expected to have somewhat distinct light-curves, some would appear relatively similar to standardizable SNe-Ia. For example, and in general, we find that for $0.2 \leq M_{\rm Ni}/M_\odot \leq 0.4$ and $0.2 \leq \zeta_{\rm sd} \leq 0.4$ a range in QNe-Ia light-curves can be found that closely overlaps our standard SN-Ia. This shows that based on (bolometric) light-curves alone, QNe-Ia could be mistaken for standard SNe-Ia. But in general QNe-Ia should deviate from the Phillips relationship. The implications to cosmology will be discussed in Section 6.3.

The peak of the light-curve in a spin-down powered QN-Ia would not be directly related to its mass (i.e. the amount of $^{56}$Ni produced) but would be sensitive to the dipole field strength and the initial period of the QS (i.e. $B_{\rm QS}$ and $P_{\rm QS}$). If QNe-Ia exist, but are mistaken for standard SNe-Ia, this additional energy input would lead to an overestimation of the amount of $^{56}$Ni produced by the explosion when using Arnett's law (Arnett 1982). Following Stritzinger & Leibundgut (2005), we can write Arnett's law as

$$L_{\rm Ni}(t_{\rm r}) = \alpha\,(6.45\,{\rm e}^{-t_{\rm r}/8.8{\rm d}} + 1.45\,{\rm e}^{-t_{\rm r}/111.3{\rm d}}) \times \frac{M_{\rm Ni}}{M_\odot} \times 10^{43}\,{\rm erg\,s^{-1}}\,, \qquad (11)$$

where $\alpha$ is a correction factor of order unity to Arnett's law and $t_{\rm r}$ is the time between explosion and maximum light (i.e., the bolometric rise time). For $\alpha = 1$ and assuming a typical SN-Ia to have a rise time of $\sim 18\,{\rm d}$ (e.g. Hayden et al. 2010; Phillips 2012), we get $L_{\rm Ni}(18\,{\rm d}) \sim 2.1 \times 10^{43}\,{\rm erg\,s^{-1}} \times M_{\rm Ni}/M_\odot$ while $L_{\rm sd}(18\,{\rm d}) \sim 2.4 \times 10^{43}\,{\rm erg\,s^{-1}} \times \zeta_{\rm sd,0.5}/(B^2_{\rm QS,15}P_{\rm QS,10})^{2/3}$ where $\zeta_{\rm sd,0.5}$ is the percentage of spin-down energy that went into radiation in units of 0.5. Since $L_{\rm Ni}(18\,{\rm d}) \sim L_{\rm sd}(18\,{\rm d})$ for our fiducial values (i.e. a total peak luminosity of $L_{\rm tot.} \sim 2\times L_{\rm Ni}(18\,{\rm d})$) this would overestimate the average $^{56}$Ni yield by a factor of up to a few. This would appear troubling since the spectrum would probably be indicative of a much lower $^{56}$Ni content (see Sect. 4.3). The spin-down energy in our model is unique and it effectively separates the photometry from the spectroscopy.

### 4.2 The Spectrum

The double-peaked structure observed in the NIR light-curves of typical SNe-Ia is a direct sign of the concentration of IPEs[3] in the central regions, whereas the lack of a secondary maximum is indicative of strong mixing. Specifically, from models of the radiative transfer within SNe, Kasen (2006) finds that the timing and strength of the shoulder is dependent on the distribution and amount of $^{56}$Ni within the ejecta. Models with a completely homogenized composition and with a small amount of $^{56}$Ni result in an $i$-band light-curve with no discernible secondary peak or shoulder. Instead, the two peaks merge to produce a single broad peak.

[3] The secondary maximum often found in $R$ and $I$ (and more prominently in the NIR) is attributed to the cooling of the ejecta to temperatures where the transition from Fe III to Fe II becomes favorable, redistributing flux from shorter wavelengths to longer wavelengths (Hoflich et al. 1995; Kasen 2006).

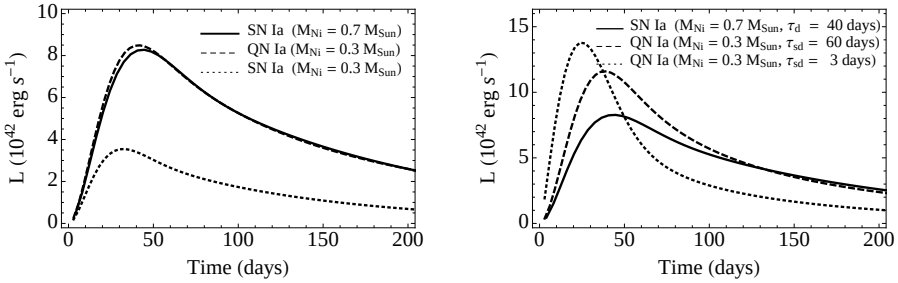


**Fig. 2** The solid line in the two panels shows the bolometric light-curve for $^{56}$Ni and $^{56}$Co decay in a standard SN-Ia model with $M_{\rm Ni} = 0.7\,M_\odot$ and diffusion time $\tau_{\rm d} = 40$ d. *Left panel*: The dashed curve shows an $M_{\rm Ni} = 0.3\,M_\odot$ QN-Ia bolometric light-curve with spin-down energy $E_{\rm sd} = 2 \times 10^{50}$ erg s$^{-1}$ (i.e. $P_{\rm QS} = 10$ ms) and $\tau_{\rm sd} = 4.5\tau_{\rm d}$ with $\tau_{\rm d} = 30$ d. For comparison a purely $^{56}$Ni-powered SN-Ia light-curve with $M_{\rm Ni} = 0.3\,M_\odot$ and diffusion time $\tau_{\rm d} = 30$ d is also shown (*dotted line*). The choices for the parameters of the $M_{\rm Ni} = 0.7\,M_\odot$ standard SN-Ia (*solid curve*) were made such that it shows close overlap with the spin-down powered QN-Ia. *Right panel*: The dashed line is a typical QN-Ia in our model (i.e. $M_{\rm Ni} = 0.3\,M_\odot$, $E_{\rm sd} = 2\times10^{50}$ erg and $\zeta_{\rm sd} = 0.5$) with $\tau_{\rm sd} = 60$ d. The dotted line is the same QN-Ia but for $\tau_{\rm sd} = 3$ d. For details on the models see Sect. 4.1.

QNe-Ia produce less $^{56}$Ni than standard luminous SNe-Ia. Thus, inherently, QNe-Ia are expected to be lacking a (or showing a weak) secondary maximum. If spin-down energy is negligible (or the energy is deposited in a jet-like structure away from the viewer's line of sight)[4], we expect spectra indicative of unmixed burning with the radioactive nickel (and thus IPEs) produced mainly in the denser core ($> 10^8$ g cm$^{-3}$) and the IMEs in the outer layers (at higher expansion velocities). These should appear in many ways (spectral features and light-curves) similar to sub-luminous SNe-Ia and should obey the Phillips relationship. However, the lack of a prominent second maximum in the $i$-band should distinguish a QN-Ia from a standard SN-Ia.

On the other hand, taking into account spin-down energy, the central overpressure caused by the energy deposition from spin-down should blow a bubble in the expanding WD material, similar to the dynamics studied in the context of pulsar wind nebulae (e.g., Chevalier & Fransson 1992). As shown in multi-dimensional calculations of pulsar wind nebulae, as the bubble expands, Rayleigh-Taylor instabilities would mix the swept-up material (e.g. Blondin et al. 2001). This could in principle occur in our case which should result in the dredging-up of burnt core material (IPEs) to the surface and IMEs to the core. This mixing should manifest itself in the presence of IPEs at higher velocity than the IMEs. Besides suppressing the $i$-band shoulder (i.e. secondary maximum), mixing will also have important implications for the spectrum, especially at late times and may affect the amount of IPEs and IMEs processed during the expansion. A more detailed analysis would require multi-dimensional studies of the coupled radiation transport and hydrodynamics, but are postponed for now.

### 4.3 Plausible QNe-Ia Candidates

Observationally, SNe-Ia have been classified into three subclasses: normal SNe-Ia, overluminous SNe (SN 1991T-like), and faint SNe-Ia (SN 1991bg-like) (Branch et al. 1993; Filippenko 1997; Li

[4] In the QN-Ia model, the spin-down source is offset from the WD explosion point by a distance of the order of $a_{\rm RL}$ (i.e. the binary separation). However, it takes only a few seconds for the WD's expanding ejecta to engulf the QS. How the spin-down energy is deposited (isotropically or with a jet-like structure) and how it is dissipated in the WD material remains to be investigated and is beyond the scope of this paper.

et al. 2001). The light-curves of more luminous SNe-Ia decline more slowly (Phillips 1993). More recently, a range of properties for peculiar subluminous SNe-Ia has been discovered:

– *SN 2006bt-like objects (broad light-curves but spectroscopically subluminous)*: Foley et al. (2010) presented evidence that SN 2006bt spectroscopically resembled SN 1991bg (subluminous, fast declining SN-Ia), but photometrically resembled a normal SN-Ia, i.e. it has a slowly-declining light-curve characteristic of a luminous SN-Ia but with spectra displaying absorption features characteristic of a low-luminosity SN-Ia. Maguire et al. (2011) presented data on the subluminous PTF 10ops which shared many similarities with SN 2006bt. PTF 10ops also had a broad light-curve. SN 2006ot appears to be related to SN 2006bt (Stritzinger et al. 2011). The photometry for this object shows that the two SNe were quite similar. This similarity also extended to the peak absolute magnitudes, which were the same to within $\sim 0.1$ mag: a broad light-curve characteristic of luminous SN-Ia ($\Delta m_{15}$(B) = 0.84 mag), but a weak secondary $i$-band maximum characteristic of low-luminosity events. Spectroscopically, however, SN 2006ot showed differences with respect to SN 2006bt although Stritzinger et al. (2011) find that at 3-4 weeks past maximum light, the spectra of SN 2006ot are similar, stressing the similarities between these two SNe.
– *SN 2003fg-like objects (overluminous but spectroscopically subluminous)*: SN-Ia 2003fg is an extremely luminous SN-Ia. Howell et al. (2006) have concluded that SN 2003fg is very likely a super-Chandrasekhar mass SN-Ia, perhaps with a mass $\sim 2\,M_{\odot}$. Other similar objects include 2006gz (Hicken et al. 2007) and SN 2007if (Akerlof et al. 2007). Despite the extreme luminosities, these SNe show the slowest luminosity evolution (i.e. low velocities of the expanding SN materials as deduced from the spectra). The low velocity and short timescale seen in SN 2003fg indicate that the ejecta mass is smaller than the Chandrasekhar mass, which is an apparent contradiction to the large luminosity.
  Maeda & Iwamoto (2009) noted that these candidate over-luminous SNe-Ia, SN 2003fg, SN 2006gz, and (moderately over-luminous) SN 1991T, have very different observational features: the characteristic timescale and velocity are very different. In analyzing SN 2003fg, Maeda & Iwamoto (2009) concluded that SN 2003fg requires that either $M_{\rm Ni}$ or $M_{\rm WD}$ (or both) should be smaller than even the Chandrasekhar mass, contrary to the earlier expectations (Howell et al. 2006). On the other hand, the large peak luminosity requires that $M_{\rm Ni} \sim 1.1\,M_{\odot}$. They also concluded that the observed features of SN 2006gz are consistent with expectations from the super-Chandrasekhar mass WD explosion scenario. They suggest that the observed differences can be attributed to different viewing orientations if the progenitor WD, and thus the SN explosion, is aspherical.
– *SN 2002cx-like objects (subluminous but spectroscopically overluminous)*: These objects have maximum-light spectra similar to those of overluminous objects like SN 1991T. However, the expansion velocities of these objects at maximum light indicate an explosion with low kinetic energy per unit mass (i.e. subluminous; Filippenko 2003; Li et al. 2003). For example, SN 2002cx had expansion velocities approximately half those of ordinary SNe-Ia. The peak absolute magnitudes in $B$ and $V$ were nearly 2 mag fainter than a normal SN-Ia of the same decline rate, and the $i$-band light-curve displayed a broad primary maximum completely lacking a secondary maximum. The distinguishing properties of SN 2002cx-like objects include: low luminosity for their light-curve shapes, a lack of a second maximum in the NIR bands, low photospheric velocities, and a host-galaxy morphology distribution highly skewed to late-type galaxies (Foley et al. 2009; Valenti et al. 2009). In general, there appears to be a great diversity among SN 2002cx-like objects, with a distribution of absolute luminosity and kinetic energy (McClelland et al. 2010).

In a very general sense, and as summarized in Figure 3, the composition, structure, and the energetics expected from spin-down powered QNe-Ia seem to resemble those inferred for the peculiar

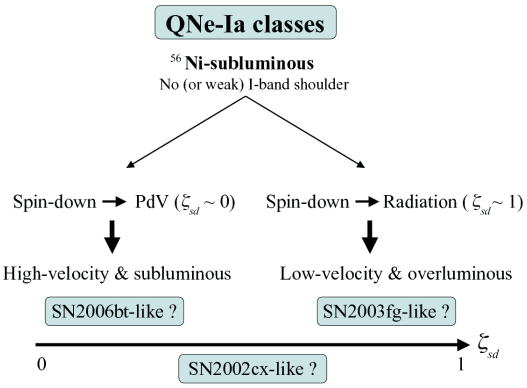


**Fig. 3** The plausible manifestations (and tentative classification) of QNe-Ia ranging from $\zeta_{\rm sd} \sim 0$ (i.e. most of the spin-down power is used during the adiabatic expansion phase; i.e. into PdV work) to $\zeta_{\rm sd} \sim 1.0$ (i.e. most of the spin-down power goes into radiation). We speculate that, and tentatively classify, SN 2006bt-like SNe as $\zeta_{\rm sd} \sim 0$ QNe-Ia, and SN 2003fg-like SNe as $\zeta_{\rm sd} \sim 1$ QNe-Ia. From the great diversity among SN 2002cx-like objects (with a distribution of absolute luminosity and kinetic energy; e.g. McClelland et al. 2010) our suggestion reflects the range in $\zeta_{\rm sd}$ which can vary from 0 to 1 in our model.

SNe-Ia objects (SN 2006bt-like, SN 2003fg-like and perhaps SN 2002cx-like). If the spin-down energy is deposited anisotropically or in a jet-like structure then QNe-Ia observed off-axis may appear as normal SNe-Ia with low $^{56}$Ni content.

Because of the spin-down energy, the photometric and spectroscopic properties of QNe-Ia are not necessarily linked to each other. In QNe-Ia the spectrum is indicative of the amount of $^{56}$Ni produced while the morphology and energetics of the light-curve can be affected (and probably dominated) by spin-down power. Depending on the initial spin-down energy (i.e. $B_{\rm QS}$ and $P_{\rm QS}$) and $\zeta_{\rm sd}$ (the percentage of the spin-down energy that went into radiation), low (high) velocities could accompany an over-luminous (sub-luminous) QN-Ia light-curve (see Fig. 3). The estimates of the photospheric velocity at the maximum brightness and of the timescale of the light-curve evolution around the peak are complicated in our model. The peculiar classes show another interesting feature: unlike standard SNe-Ia with similar decline rates, they seem to be lacking a prominent second maximum in the $i$-band; the ejecta in these objects seems to be well mixed. The low $^{56}$Ni yields in QNe-Ia and the efficient mixing likely to be induced by the pulsar-wind bubble provide conditions to erase (or at least minimize) the $i$-band shoulder.

### 4.4 Summary

The exact shape of a QN-Ia light-curve taking into account the spin-down power remains to be computed (in particular in the $B$-band) for a more robust comparison to a standard light-curve. For now we would argue that spin-down powered QNe-Ia should be associated with fairly broad light-curves with rise and decay time phases that should somewhat deviate from $^{56}$Ni-powered (i.e. standard) light-curves (see Fig. 2). However while QNe-Ia would be associated with somewhat distinct light-curves, some would still appear similar to standard ones. In the QN-Ia model, the additional (spin-down) power source effectively separates photometry from spectroscopy. The $M_{\rm Ni}$ yield and the kinetic energy are not necessarily linked which means that the expansion velocities in QNe-Ia are not indicative of how powerful the explosion is.

## 5 THE BINARY PROGENITOR

We ask what progenitor could lead to a tight MNS-COWD system experiencing the QN event after it has settled into $a \sim a_{\rm RL}$? In others words a necessary condition is for $\tau_{\rm QN}$ to exceed the time it takes the MNS-COWD, from the moment of its birth, to shrink its orbit to $a = a_{\rm RL}$. A non-accreting NS-WD system, born with an initial period $P_0$, sees its orbit shrink due to GW emission. The orbital period decay rate, neglecting orbital eccentricity, is $dP/dt = -1.03 \times 10^{-7}\ {\rm s\,s^{-1}}\ (2\pi/P)^{5/3} \times (M_{\rm NS,\odot} M_{\rm WD,0.6})/M_{\rm T,\odot}^{1/3}$ (Landau & Lifshitz 1975). A solution is $P(t) = P_0 \times (1 - t/\tau_{\rm GW})^{3/8}$ with

$$\tau_{\rm GW} \sim 10^7\ {\rm yr}\ \frac{P_{0,\rm hr}^{8/3} M_{\rm T,\odot}^{1/3}}{M_{\rm NS,\odot} M_{\rm WD,0.6}}\ , \tag{12}$$

and $P_{0,\rm hr}$ being the initial period (in hours). Here $M_{\rm T,\odot}$ is the total mass in solar units.

Any interacting binary (with a primary $M_{\rm prim}$ and a secondary $M_{\rm sec}$) that leads to an MNS-COWD system with $M_{\rm NS} \sim M_{\rm NS,c}$ and a WD that has filled its RL is a potential candidate. The accretion from the WD onto the NS will eventually drive the NS above $5\rho_{\rm N}$ triggering a QN event. However, there is also the possibility of the NS being born with $M_{\rm NS} > M_{\rm NS,c}$ but in a fully recycled state ($P_{\rm NS} < 2$ ms) so that its core density is below the critical value. This case, which we refer to as scenario 1 (hereafter S1), is discussed first then followed by scenario 2 for a mildly recycled case ($10\,{\rm ms} < P_{\rm NS} < 100\,{\rm ms}$; hereafter S2). S1 and S2 involve a direct formation of the NS by iron-core collapse with one of the binary components being massive enough to lead to an MNS. There is also an indirect path to forming an NS in a binary which appeals to the AIC of a WD to an NS (we will refer to this as S3; scenario 3). Mass transfer can drive a WD in a binary over the Chandrasekhar limit, which may lead to an AIC (in the case of an ONeMg WD; and possibly also in some CO WDs) which produces an NS. This is the most interesting one if it can be shown that a massive enough NS can result from the AIC of the WD.

The mass of the progenitor star that could lead to an MNS (prone to the QN transition) is in the $20 - 40\ M_\odot$ range. For this range, the QNe rate is estimated to be $\eta_{\rm QN} \leq 1/100$ core-collapse (CC) events ($\eta_{\rm QN} < 0.01\eta_{\rm CC}$; Jaikumar et al. 2007; Leahy & Ouyed 2008; Leahy & Ouyed 2009; Ouyed et al. 2009). Assuming that 1/10 occur in tight binaries as required here, this means a QN-Ia rate $\leq 1/1000$ core-collapse events in this scenario. This is lower than the currently observed rate for Type Ia, which is $\sim 1/10$ of core-collapse SNe (e.g. Pritchet et al. 2008 and references therein). Unless the NS gains mass during the binary evolution towards the tight MNS-COWD system, both S1 and S2 will be plagued by low statistics (i.e. direct dependency on $\eta_{\rm QN}$). However, a top-heavy IMF of Pop. II stars together with a boost in star formation rate at early times could make QNe-Ia from S2 statistically significant at high redshift. The AIC channel yields better statistics provided enough of them lead to NSs which undergo a QN explosion. Below we briefly describe each scenario.

### 5.1 MNS-COWD Systems with Fully Recycled NSs

The need for a COWD in our model and the requirement of a fully recycled NS hint at IMXBs: (i) with a donor star in the $3.5\,M_\odot < M_{\rm don} < 5\,M_\odot$ range; (ii) and have undergone a substantial accretion phase (e.g. Tauris et al. 2000). In particular, IMXBs evolving via the so-called "Case A Roche-Lobe Overflow (RLO)" phase[5], that evades spiral-in, go through a mass-transfer phase lasting

[5] There are three types of RLO (e.g. Tauris et al. 2000; Podsiadlowski et al. 2002): cases A, B and C. In case A, the system is so close that the donor star begins to fill its Roche-lobe during core-hydrogen burning: in case B the primary begins to fill its Roche-lobe after the end of core-hydrogen burning but before helium ignition: in case C it overflows its Roche-lobe during helium shell burning or beyond. Cases B and C occur over a wide range of radii (orbital periods); case C even up to orbital periods of about 10 yr. The precise orbital period ranges for cases A, B, and C depend on the initial donor star mass and on the mass ratio (see Tauris 2011). Once the RLO has started, it continues until the donor has lost its hydrogen-rich envelope (typically $> 70\%$ of its total mass) and subsequently no longer fills its Roche-lobe.

about $10^7$ yr. These mainly lead to millisecond pulsars (MSPs) with CO WD companions. This evolutionary path provides enough material to spin-up a slowly rotating NS to an MSP. Furthermore, the magnetic field of the MSP would have decayed in the process due to accretion (Taam & van den Heuvel 1986). Assuming the MSPs were born with an initial magnetic field of $\sim 10^{12}$ G, accretion would decrease its surface magnetic field to $\sim 10^9$ G ($\sim 10^8$ G) by accreting only a few hundredths to a few tenths of $M_\odot$. This means $\tau_{\rm QN} < 10^8 (< 10^{10})$ yr for the cases of EoSs considered here.

The necessary condition we seek translates to $\tau_{\rm QN} > \tau_{\rm GW}$ which yields $P_0 < 2.4 \ {\rm h} \times \tau_{\rm QN,8}^{3/8} (M_{\rm NS,\odot} M_{\rm WD,\odot})^{1/3} / M_{\rm T,\odot}^{1/8}$ (for $\tau_{\rm QN} = 10^8$ yr). Thus only NS-WD systems born with periods $P_0$ in the range of a few hours can be considered serious candidates for QNe-Ia in this scenario. However, evolution calculations of relevant IMXBs show that for a progenitor mass range of $3.5 < M_{\rm don}/M_\odot < 5$, the final binary periods are days instead of hours (Tauris et al. 2000). It might be the case that IMXBs which lead to QNe-Ia are those that have experienced additional angular momentum loss (i.e. orbit shrinkage). An interesting possibility is that a small fraction of the transferred mass from the donor forms a circumbinary disk (CD). Evolution calculations in the context of Cataclysmic Variables (Spruit & Taam 2001) and Black Hole IMXBs (Chen & Li 2006) show that systems with an initial period of a few days reach final orbital periods of a few hours when a CD (which enhances the mass-transfer rate) is taken into account. In principle we expect similar results for IMXBs described here if CDs are involved. Systems with CDs require additional angular momentum loss which is not considered in our model. Further studies on the evolution of such IMXBs are needed.

While we do not expect QNe-Ia via S1 to be very common in today's universe (if these are related to $\eta_{\rm QN}$), it might have been different in the early universe where a boost in star formation rate has been suggested. An order of magnitude estimate of QN-Ia rate for this path is $\eta_{\rm QN-Ia} \sim \epsilon_{\rm IMXB} \times \eta_{\rm cc,0} \times \alpha_{\rm SFR}$ where $\eta_{\rm cc,0}$ is the current core-collapse rate and $\alpha_{\rm SFR}$ is the boost in star formation rate at $1 < z < 2$. Here $\epsilon_{\rm IMXB} \sim \epsilon_{\rm IMXB,CC} \times \epsilon_{\rm IMXB,QNIa}$ where $\epsilon_{\rm IMXB,CC}$ is the fraction of CC which leads to an IMXB (of the order of $10^{-3}$; Pfahl et al. 2003), while $\epsilon_{\rm IMXB,QNIa}$ is the percentage of IMXBs experiencing a QN-Ia. Assuming the current SD rate to be $\eta_{\rm SD,0} \sim \eta_{\rm cc,0}/10$, we get $\eta_{\rm QN-Ia} \sim \epsilon_{\rm IMXB,QNIa} \times \eta_{\rm SD,0} \times \alpha_{\rm SFR,100}$ where $\alpha_{\rm SFR,100}$ is in units of 100. The QN-Ia rate would exceed the SD rate, $\eta_{\rm SD}$, if $\epsilon_{\rm IMXBs,QNIa} \geq 1 \times \eta_{\rm SD}/\eta_{\rm SD,0}$. For QNe-Ia to be significant (compared to the SD channel) at high redshift, we require $\epsilon_{\rm IMXB,QNIa} \sim 1.0$ which means that virtually all IMXBs should lead to QNe-Ia.

In summary, unless the SD rate decreases drastically at higher redshift (i.e. $\eta_{\rm SD} \ll \eta_{\rm SD,0}$), it remains a challenge for QNe-Ia in this scenario (i.e. S1) to become statistically significant at any time. Furthermore, CDs of the mass required in our model have yet to be confirmed observationally (e.g. Muno & Mauerhan 2006). Another downside to this scenario is the $\tau_{\rm QN} \gg \tau_{\rm GW}$ regime, if most NSs end up with a magnetic field that is too small ($\leq 10^8$ G). This case cannot be excluded and it would imply that the available time window for a QN to occur when the system is still at $a = a_{\rm RL}$ is even shorter.

### 5.2 MNS-COWD Systems with a Mildly Recycled NS

The second scenario (namely, S2) is that of a tight binary system with the NS born massive (ideally close to $M_{\rm NS,c}$) but not necessarily fully recycled (see sect. 3.7 in van den Heuvel 2011 for an explanation of massive NSs in binaries). In this case, as long as the NS does not accrete as the system evolves towards $a_{\rm RL}$, the QN explosion will most likely occur shortly after the WD overflows its RL, driving the NS mass (or core density) above $M_{\rm NS,c}$ (above the deconfinement value). This means that $\tau_{\rm QN} \sim \tau_{\rm WD}$ in S2 which is a more universal and realistic result since it is independent of the NS's initial period and magnetic field.

It is well-known that an NS+COWD system with a non-fully recycled NS can form in a very tight binary via a Common Envelope (CE) (e.g. Ferdman et al. 2010). Since most NS+CO tight

binary systems form via the CE phase, this scenario provides better statistics for the QN-Ia rate than the fully recycled NS one. Still, this would require that an important percentage of these lead to MNS via accretion. So far it appears that MNSs in CE channels must have been born massive (e.g. Tauris et al. 2011) in which case their statistics would be tied to $\eta_{\rm QN}$ instead of $\eta_{\rm CC}$.

### 5.3 The Accretion-Induced-Collapse Scenario

The possibility of merging in CO WDs as SNe-Ia progenitors has been investigated (see Livio 2000 for a review). The outcome of these simulations is an inward propagating flame that converts the accreting CO WD into an ONeMg WD. This star is gravitationally unstable and undergoes an AIC[6] to form an NS (e.g. Nomoto & Iben 1985; Saio & Nomoto 1985; Fryer et al. 1999). Modern simulations of WD-WD mergers suggest that AIC is the most likely outcome (e.g. Saio & Nomoto 2004; Yoon et al. 2007). If a Type I supernova is to follow from merging WDs, a thick disk must be formed as an intermediate stage in the merging process, with transfer from the disk onto the central degenerate dwarf occurring at a rate sufficiently less than Eddington that a deflagration induced by carbon burning occurs. Thus, the outcome of the merging of two massive CO degenerate dwarfs is not trivially a Type I supernova explosion. Detailed 2-dimensional axisymmetric simulations of AIC (Dessart et al. 2006, 2007) find that the AIC of a WD forms a $\sim 1.4-1.5\ M_\odot$ NS, expelling a modest mass of a few $10^{-3}\ M_\odot$ mostly through a neutrino-driven wind. A quasi-Keplerian accretion CO-rich disk with mass $\sim 0.1-0.5\ M_\odot$ forms around the newly-formed proto-NS.

The AIC of a WD to a NS releases significant binding energy. The gravitational mass of the resulting NS is the Chandrasekhar mass minus the gravitational binding energy of the NS. Typically assumed numbers are that an accreting ONeMg WD, if pushed to AIC (at a mass of $1.44\ M_\odot$), leaves behind a $1.25\ M_\odot$ NS. In this context, the feasibility of a QN-Ia relies heavily on: (i) the formation of a very massive $> 1.3\ M_\odot$ ONeMg WD; (ii) subsequent rapid accretion onto the $\sim 1.25\ M_\odot$ NS following AIC of the ONeMg WD; (iii) a companion that should provide enough mass to first trigger the AIC then to increase the NS mass from $\sim 1.25\ M_\odot$ to $M_{\rm NS,c}$ and eventually evolve into a CO WD.

Let us consider a WD-WD system which consists of an ONeMg WD close to the $1.44\ M_\odot$ and a donor CO WD. Since the AIC of the ONeMg WD leads to an $\sim 1.25\ M_\odot$, the donor companion must be massive enough to provide enough mass to push the NS to $M_{\rm NS,c}$ and leave behind a CO WD. Taking into account the binding energy lost during accretion from the companion, it is hard to imagine how accretion from an $\sim 0.6\ M_\odot$ WD companion can push the NS to even the very low critical mass of $1.6\ M_\odot$, making the QN unlikely[7]. The need for a massive donor WD ($\gg 0.6\ M_\odot$) means that the mass ratio is sufficiently high that the two systems will merge. If it turns out that such a merger leads to an MNS engulfed in a degenerate CO-rich torus (e.g. Yoon et al. 2007), then a QN-Ia is a possibility; although this case violates the $q \leq 0.5$ constraint of our model, we consider it here for completeness.

There is one more channel worth mentioning. Belczynski & Taam (2004) find that even if the ONeMg WDs were formed at a reasonably lower mass ($\sim 1.2\ M_\odot$), some would still be pushed over the Chandrasekhar mass limit[8]. They argue that the last CE episode results in the formation of not only WD ($\sim$40%) but also low-mass He star ($\sim$40%) secondaries (see Table 1 in Belczynski & Taam 2004). Either the WD or the helium star companion fills its Roche lobe and starts transferring material to the ONeMg WD. The AIC interrupts the mass transfer because of the loss of binding

[6] Accreting CO-ONeMg systems where the ONeMg WDs may have formed directly from an $\sim 8-10\ M_\odot$ progenitor star are also viable candidates for QNe-Ia.

[7] See however Xu (2005) for alternative mechanisms for the formation of quark stars via the AIC channel.

[8] The formation of massive ONeMg WDs might be challenging for a single star channel; the initial-final mass relationship derived by Meng et al. (2008) suggests that massive ONeMg WDs may only form for single stars at significantly super-solar metallicities (which means mostly in today's universe).

energy of the collapsing dwarf. However, in the case of a helium star donor, mass transfer may restart on a short timescale, as nuclear expansion of the helium star is faster in bringing the system into contact than gravitational waves in the case of a WD donor. The helium star donors eventually lose sufficient mass to become low-mass hybrid WDs (with carbon/oxygen in the core surrounded by helium).

In principle, the helium star donor channel could lead to an AIC of a massive ONeMg WD while providing a sufficient mass reservoir to form a massive enough NS to undergo a QN (see also Taam 2004 and references therein). The helium-donor case is the preferred scenario if the resulting low-mass hybrid WD could undergo a detonation following impact by the QNE (i.e. if compression is high enough to achieve WD densities $> 2.5 \times 10^7$ g cm$^{-3}$ and trigger burning under relativistic degenerate conditions).

As a subset of AIC, the rate of QNe-Ia via this channel depends on the AIC rate. However, because AIC has never been observationally identified, its rate is uncertain. Theoretical estimates of the rate of AICs are also quite uncertain. Based on r-process nucleosynthetic yields obtained from previous simulations of the AIC of WDs, Fryer et al. (1999) inferred rates ranging from $\sim 10^{-5}$ to $\sim 10^{-8}$ yr$^{-1}$ in a Milky-Way-sized galaxy. This result depends upon a number of assumptions and the true rate of AICs could be much lower or much higher than this value. If higher numbers can be confirmed, then a small percentage of AICs leading to MNSs (with the subsequent QNe explosions under conditions described above) could make QNe-Ia statistically viable.

A population that is close to the NS-WD systems described here is the "Ultra-Compact X-ray binaries" that contain CO WDs (e.g. Nelemans et al. 2010). These have most likely evolved via the CE with the WD probably sitting at $a_{\rm RL}$. In particular if it can be shown that some UCXBs contain a MNS then these would be potential QNe-Ia candidates. These, we will investigate elsewhere.

### 5.4 Summary

To summarize this section, we have presented three possible progenitors of QNe-Ia. S1 and S2 appeal to IMXBs that lead to a tight MNS-COWD binary. S1 and S2 are related to massive star formation (rate) while S3 is related to slightly lower mass star formation (since the NS forms from the AIC of a WD). We find the S1 scenario (fully recycled NS) the least likely progenitor not only because of its extremely rare occurrence but also because of the constraint it imposes on the MNS-COWD birth period ($P_0$ much less than a few hours). S2 should be considered a serious option if the Pop. II IMF favored more massive stars. There is also the intriguing possibility of the AIC channel (S3) which might be the most viable statistically if the AIC rate is indeed very high; which remains to be confirmed. S2 and S3, we argue, lead to relatively prompt explosions (with delay time $t_{\rm delay}$ not exceeding a few Myrs; see Sect. 6.2) while S1 would lead to a longer time delay. We mention that if it happens that mergers occur at smaller values of $q$ than considered here (i.e. $q < 0.5$), then S1 and S2 would be less likely since these depend heavily on stable mass-transfer; only S3 would remain as a viable QN-Ia progenitor. Much uncertainty still remains regarding the formation and evolution of close binary stars, in particular those evolving through a CE phase and/or a WD-WD path. However, if any of these scenarios could lead to tight (i.e. with $a \sim a_{\rm RL}$) MNS-COWD systems with NS masses close to $M_{\rm NS,c}$ then we might have at hand a viable channel for QNe-Ia.

Despite these uncertainties, we mention that binary evolutionary paths exist that could lead to compact binary systems with an MNS and a CO WD as described above. For example, the evolutionary path C shown in figure 1 in Stairs (2004) leads to a binary system closely resembling PSR J1141−6545 with an NS mass of $1.3\,M_\odot$ and a WD mass of $1\,M_\odot$ (see table 1 in Stairs 2004). This system has a birth period of 0.2 d which is within the conditions described for the S1 scenario above. Another candidate that could potentially evolve to an S1 case is PSR J1802−2124 which consists of a $\sim 1.24\,M_\odot$ mildly recycled ($\sim 12.6$ ms) NS and a $\sim 0.78\,M_\odot$ WD (Ferdman et al. 2010).

Accretion onto the NS could in principle increase its mass to $M_{\rm NS,c}$ (i.e. recycling it) and trigger a QN event and subsequently a QN-Ia.

## 6 DISCUSSION

### 6.1 Other Sub-Chandrasekhar Models

As discussed in the Introduction, sub-Chandrasekhar models can be classified as: (i) edge-lit (with a helium layer) single-degenerate sub-Chandrasekhar mass explosions (Woosley & Kasen 2011); core-lit (without a helium layer) single-degenerate sub-Chandrasekhar mass explosions (Sim et al. 2010); (iii) core-lit sub-Chandrasekhar mass remnants from mergers of roughly equal-mass CO WDs (van Kerkwijk et al. 2010). These involve $> 0.9\,M_\odot$ WDs and are all powered purely by $^{56}$Ni decay. The lower mass WDs in these models mean a deflagration might not necessarily produce the observed IMEs. Some are more successful in reproducing observed SNe-Ia than others.

There are fundamental differences between our model and those described above, which can be summarized as follows. (i) The compression and heat deposition induced by the impact of the QNE puts the WD in a regime "mimicking" massive WDs ($\rho_{\rm SWD} > 10^8$ g cm$^{-3}$) despite the much lower mass WD involved ($M_{\rm WD} < 0.9\,M_\odot$). Our model involves truly sub-Chandrasekhar mass WDs at explosion. As we argued in Section 3.2, the shock from the QNE impact could in principle reach deep into the WD core to trigger an inside-out (i.e. a centrally ignited) explosion; (ii) In our case no helium layer is necessary, i.e. the explosion is independent of accretion onto the WD. Nevertheless, as discussed in Section 5.3, one of the AIC channels would lead to an MNS surrounded by a hybrid HeCO WD. If these systems experience a QN explosion of the MNS then they would have some distinct (photometric and spectroscopic) properties given the extremely low-mass WD ($< 0.3\,M_\odot$) and the presence of helium. (iii) The additional energy source (i.e. the spin-down power) would affect the evolution of the fireball and the resulting light-curve.

### 6.2 The Connection to Star Formation?

SNe-Ia are seen to occur in early type (elliptical) galaxies and in younger stellar populations. Observations have shown that they are more prevalent in star-forming late-type galaxies than in early-type galaxies (Oemler & Tinsley 1979). Young galaxies host roughly two times more SNe-Ia than early-type galaxies (Nomoto et al. 2000) because SNe-Ia are slightly more efficiently produced in younger stellar populations (Bartunov et al. 1994). The mean luminosities of SNe-Ia observed in spiral galaxies are clearly higher than those of elliptical galaxies (Wang et al. 2008). A very significant factor here is the absence of the brightest SNe-Ia in elliptical and S0 galaxies. The current explanation for these observations is that there are prompt (delayed by $\sim 200$ to $\sim 500$ Myr from the onset of star formation; Oemler & Tinsley 1979; Raskin et al. 2009) and delayed (tardy, $> 1$ Gyr) SN-Ia explosions (e.g. Ruiter et al. 2009 and references therein). The prompt component is dependent on the rate of recent star formation, and the delayed component is dependent on the total number of low-mass stars. The combination of these two components is believed to form the overall observed SN-Ia rate (Hamuy et al. 2000; Sullivan et al. 2006; Wang et al. 2008; Sullivan et al. 2010).

In S2 and S3, QNe-Ia might occur shortly after star formation with a delay associated with the donor's main-sequence lifetime. Specifically, $t_{\rm delay} \simeq \tau_{\rm M_2} + \tau_{\rm GW} \simeq \tau_{\rm M_2} \sim 3 \times 10^8$ yr $(4\,M_\odot/M_2)^{2.5}$ which gives[9] 70 Myr $< t_{\rm M_{delay}} <$ 300 Myr; this assumes $\tau_{\rm QN} \sim \tau_{\rm GW} < \tau_{\rm M_2}$.

[9] Mass exchange during the binary evolution makes it hard to pin-point the exact range of WD progenitor mass. However, in our model this exchange may be minimal given the mass of the primary ($20\,M_\odot < M_{\rm prim} < 40\,M_\odot$; for the S2 channel) required to form a massive NS at birth. The primary would explode as an SN very shortly after the binary's formation. In this case we do not expect much interaction and mass exchange with the secondary until it evolves to the red giant phase. For a $\sim 0.6\,M_\odot$ WD this justifies the secondary's mass range we adopt of $4\,M_\odot < M_2 < 7\,M_\odot$ (e.g. Tauris 2011).

A burst in massive star formation at high redshift combined with a slightly heavier IMF of Pop. II stars would increase the formation rate of MNSs and also probably of massive CO WDs. The increase in massive CO WDs could lead to an increase in ONeMg WD numbers via accretion processes described in Section 5.3 (at high-redshift and low-metallicity, direct formation of ONeMg WDs from single stars is heavily reduced; Meng et al. 2008). The suggested peak in star formation rate at redshifts $1 < z < 2$ (e.g. Hughes et al. 1998; Madau et al. 1998; Pettini et al. 1998; Dickinson et al. 2003) combined with a heavier IMF of Pop. II stars would make the S2 and S3 channels highly plausible and may be prominent in the early universe. This means that the QN-Ia rate could peak at $0.75 < z < 1.75$ if they occur on average $< 300$ Myr after the onset of star formation (Wright 2006). However, the rate estimates given in this work are still subject to substantial uncertainties.

### 6.3 Plausible Implication to Cosmology

SNe-Ia have been successfully used as standardizable (Phillips 1993) distance candles and have provided the first indication for an accelerating Universe and the need for dark energy (Riess et al. 1998; Perlmutter et al. 1999). Effectively, they provided evidence for a universe that experiences an accelerated expansion since the time when it was about half of its present age. At that time, the predicted dark energy took over the kinematics of our universe that was ruled by the matter contribution before. This conclusion was based on a sample of over a hundred nearby SNe-Ia that have been studied, revealing considerable homogeneity. However some fascinating differences between SNe-Ia do exist (e.g. Phillips 2012) and in particular for those interested in using SNe-Ia as cosmological distance indicators, the most troubling of the peculiar objects are the 2006bt-like SNe.

SN 2006bt was observed to have a fairly broad, slowly decaying light curve, indicative of a luminous supernova. However, it displayed intrinsically-red colors and optical spectroscopic properties that were more like those of fast-declining, low-luminosity events (it was also lacking the $i$-band shoulder). Although SN 2006bt appears to have a somewhat odd light curve, it is still a relatively good standardizable candle. The intrinsically-red color evolution of the SN caused standard light-curve fitting programs to significantly overestimate the dust reddening[10]. This happened, despite the fact that SN 2006bt occurred in the outskirts of a galaxy, showing no sign of dust absorption. All light-curve fitters correct for its red color by effectively brightening its apparent magnitudes. This brightening correction followed by standard calibration techniques could either over-estimate or under-estimate the true magnitude. Foley et al. (2010) developed a Monte Carlo simulation to assess the impact of contamination of a population of SN 2006bt-like objects in an SN-Ia cosmological sample. Using basic simulations, they showed that SN 2006bt-like objects can have a large impact on derived cosmological parameters. As can be seen from their figure 12, a 10% contamination of SN 2006bt-like objects, in the nearby ($z < 0.1$) and full samples, increases the scatter of an SN-Ia Hubble diagram and systematically biases measurements of cosmological parameters (see also their Table 3).

We have already noted the intriguing similarities between SN 2006bt-like (and other peculiar SNe-Ia) objects and QNe-Ia (see Sect. 4.3). In particular we noted and showed that some QNe-Ia light-curves could be mistaken for standard SNe-Ia of higher $^{56}$Ni content (see Fig. 2). Since photometry and spectroscopy are not necessarily linked in QNe-Ia, light-curve fitters would be confused by these. They would apply brightening corrections and standard calibration techniques that could either over-estimate or under-estimate the true magnitude of these QNe-Ia. Once the QN-Ia light-curve is derived/computed in detail, a study similar to Foley et al. (2010) should be performed in order to assess plausible QNe-Ia contamination and the implication for the SN-Ia Hubble diagram. For now, if the analysis of Foley et al. (2010) were any indication, we are tempted to speculate

[10] Light-curve fitters must correct for the fact that redder supernovae are dimmer. This is due to a combination of an intrinsic color-luminosity relation (faint supernovae are intrinsically red; Riess et al. 1996), and reddening due to dust.

that QNe-Ia if they exist (in particular at high redshift) might systematically bias measurements of cosmological parameters.

Are QNe-Ia contaminating the high-redshift SNe sample? Observations show that the most luminous SNe-Ia (those with the broadest lightcurves) favor star forming hosts and occur only in late-type galaxies (Hamuy et al. 1996). Since star formation increases by a factor of 10 up to redshift 2 (e.g. Hughes et al. 1998; Madau et al. 1998; Pettini et al. 1998; Dickinson et al. 2003), it is expected that the mix of supernovae will change with redshift. Howell et al. (2007) find the fraction of broad light-curve SNe increases with redshift and seems to agree with the idea that as star formation increases with redshift, so the broader light-curve SNe-Ia associated with a young stellar population make up an increasingly larger fraction of SNe-Ia. We have already argued that spin-down powered QNe-Ia should be associated with bright and broad light-curves and should be linked to star forming regions (the delay time between formation and explosion should not exceed a few Myrs for S2 and S3; see Sect. 6.2) which means they should exist at high $z$. In particular, QNe-Ia with $\zeta_{\rm sd}$ closer to 1 would be extremely luminous and should be easily detected (if not dominant) at high redshift. In addition, as mentioned in Section 6.2, a burst in massive star formation at high redshift combined with a slightly heavier IMF of Pop. II stars would increase the formation rate of MNSs and also probably that of massive CO WDs. The increase in the mass of CO WDs could, overall, make QNe-Ia at high-redshift produce more $^{56}$Ni which should increase their brightness.

If observed luminous high-redshift SNe (or at least a percentage of them) are truly luminous QNe-Ia (i.e. powered by spin-down), then these should be removed from the sample before calibrations[11] are made. Unfortunately, at such high-redshift (in fact for any SN at $z > 0.3$), the $i$-band is redshifted out of the optical, thus making the identification as QNe-Ia very challenging. Nevertheless, one could in principle rely on unique features of QNe-Ia light-curves and spectra to differentiate between $^{56}$Ni powered SNe and QNe-Ia at high-redshift (see Sect. 7). If not, then if QNe-Ia were to account for a percentage (perhaps as low as $\sim$ 10%) of the SN-Ia sample at high-redshift (in our rough estimates at $0.5 < z < 1.75$), one wonders if these could systematically bias measurements of cosmological parameters that could allow for other cosmologies, and possibly explain away the need for dark energy? This is of course a daring and highly speculative conclusion since it ignores the constraints from the "concordance model"[12] (see however Kroupa et al. 2010).

## 7 PREDICTIONS AND CONCLUSIONS

We proposed a new model for Type Ia SNe involving a QN going off in a tight MNS-COWD binary. The impact of the dense relativistic QNE on the WD could lead to compression and heating which, under appropriate conditions, should lead to the ignition and detonation of the WD, thus causing the QN-Ia. A particularity of our model is the spin-down power from the QS (the QN compact remnant) which provides an additional energy input (besides the $^{56}$Ni decay) to make the QN-Ia fairly bright. Our preliminary calculations of QNe-Ia light-curves suggest that these should somewhat deviate from the Phillips relationship although some are close enough to standard (i.e. $^{56}$Ni-powered) SNe-Ia that they could easily be confused as such. Another particularity of our model is that the photometric and spectroscopic properties are not necessarily linked. Light-curve fitters "stumbling on" a QN-Ia would find a discrepancy between the light-curve and the spectrum at peak and would try to correct for it by incorrectly brightening or dimming the object. This, we argue, could systematically

[11] If these were powered purely by $^{56}$Ni decay then this mixing is not necessarily problematic for cosmology since light-curve shape, color correction and correction for host galaxy properties allow all supernovae to be corrected to the same absolute magnitude; thus avoiding systematic residuals with respect to the Hubble diagram.

[12] The values of $\Omega_\Lambda$ and $\Omega_{\rm M}$ are confirmed also from the examination of the cosmic microwave background (CMB) and galaxy clusters. The consistence of these three methods is known as Cosmic Concordance. The position of the first Doppler peak as well as the comparison of the peak amplitudes for different multipole moments in the CMB angular power spectrum indicates a flat Universe and constrains the sum of $\Omega_{\rm M}$ and $\Omega_\Lambda$ (e.g. Spergel et al. 2003 and references therein). $\Omega_{\rm M}$ is constrained by the evaluation of the mass of galaxy clusters (e.g. Carlberg et al. 1998).

bias measurements of cosmological parameters if QNe-Ia at high-redshift are numerous and bright enough to be included in the cosmological sample.

Some features/predictions of our model are:

(i) We start by pointing out that we expect the QN proper to be much less luminous (in the optical) than the QN-Ia. Most of the QN energy is in the kinetic energy of the QNE so unless the QNE interacts strongly with its surroundings it will not be optically bright; the QN will be dwarfed (in the optical) by the QN-Ia given the low-density expected in the binaries considered here. In much denser environments, the collision between the QNE and the surroundings leads to extremely bright QNe (Leahy & Ouyed 2008; Ouyed & Leahy 2012).

(ii) Given the QNE kinetic energy ($\sim 10^{52}$ erg), QNe-Ia should be associated with cavities (i.e. they would carve out bubbles) much larger than those expected from Type IIs and standard Type Ias.

(iii) The expanding neutron-rich QN ejecta would have processed mostly heavy elements with atomic mass $A > 130$ (Jaikumar et al. 2007). The $\sim 10^{-3}\ M_{\odot}$ in the QN ejecta provides a substantial amount of $A > 130$ to contaminate their environment (and thus QNe-Ia environments) with such elements.

(iv) The nature of the GW signal from a QN has been computed in Staff et al. (2012). Prior to the QN explosion proper, the NS-WD objects described here would also be a source of detectable signals since we expect them to be more common than NS-NS and/or NS-BH systems. As expected, GW signals from SD and/or DD channels would be distinct from those from QNe-Ia. In the QN-Ia model, we expect a delay between the GWs signalling the QN proper and the GWs signalling the explosion of the WD. The delay is of the order of a fraction of a second and is a combination of the time it takes the QNE to reach the WD and the burning time of the WD.

(v) Unlike other models of SNe-Ia so far proposed in the literature, the QN leaves behind a compact star. The compact remnant, in our model, would be a radio-quiet quark star (an aligned rotator; Ouyed et al. 2004 and Ouyed et al. 2006) with specific X-ray signatures (Ouyed et al. 2007a,b).

(vi) The spin-down luminosity of the resulting quark star (Staff et al. 2008) would result in the formation of a wind nebula (much like a pulsar-wind nebula) which is another unique feature of our model. Association of an SN-Ia with a pulsar-wind nebula would strongly support our model. In particular, given the similarities between QNe-Ia and peculiar SNe-Ia (see Sect. 4.3), it would be interesting to search for signatures of a pulsar-wind nebula (or even extremely large cavities) in peculiar SNe-Ia. One could search for possible signatures of any asymmetries in the propagating ejecta, e.g. by using polarization measurements taken at early times (prior to maximum light; e.g. Wang & Wheeler 2008).

(vii) If the high-redshift SNe-Ia are truly spin-down powered QNe-Ia, these would lack (or show a weak) second maximum in the $i$-band. Although the $i$-band would be shifted from the optical, one could in principle perform this exercise in the infrared (which should be within the JWST's reach at $z \sim 1$).

(viii) Applying Arnett's law to a QN-Ia, as we have said, would lead to an overestimation of the true $^{56}$Ni yield. In QNe-Ia, the $^{56}$Co yield one would infer from the later times ($\gg 8.8$ d) would be much smaller than those obtained around the peak.

(ix) Finally, we suggest a few QNe-Ia candidates among historical Galactic Type-Ia remnants. According to predictions in the SD models, the companion star (i.e. the donor star) should survive the explosion and thus should be visible in the center of Type Ia remnants. A direct detection of a surviving donor star in a Galactic Type Ia remnant would substantiate the SD channel for at least one system. Among the known Galactic remnants (e.g. Tycho Brahe's SN, Kepler's SN, SN 1006), none shows the undeniable presence of a surviving companion. For example, the well studied case of SN 1006 seems to be lacking a surviving donor star (Kerzendorf

et al. 2012; González Hernández et al. 2012). Recently, Schaefer & Pagnotta (2012) reported that the central region of the supernova remnant SNR 0509−67.5 (in the Large Magellanic Cloud) lacks an ex-companion down to very faint magnitudes. While the DD scenario might be an alternative progenitor[13], we argue that for those remnants where the SD can be ruled out through deep imaging observations, i.e. those with a clear lack of any ex-companion star, the QN-Ia avenue should also be explored.
SN 1006 and SNR 0509−67.5 are particularly interesting and should be considered potential QN-Ia contenders. If future deep monitoring of these systems reveals a radio-quiet[14] compact remnant (the QS) emitting in the X-rays then one can make a strong case for a QN-Ia. Another clue to look for is a cavity carved out by the QN ejecta prior to the QN-Ia; in our model, the QN explosion proper (which explodes first) creates the cavity into which the WD explodes following impact from the QNE. In this context, we should mention another historical remnant of interest to our model namely, RCW 86. A self-consistent explanation of the infrared, X-ray, and optical observations in this object presumably requires an explosion into a cavity created by the progenitor system (Williams et al. 2011). This hints at the SD channel where the progenitor might have carved a wind-blown bubble. However, if future measurements can rule out a main-sequence or a giant companion in RCW 86, then this would lend support to the QN-Ia assuming that wind-blown bubbles cannot be formed in DD models or in SD models in general.

To compare to detailed observations, it is necessary to perform detailed multi-dimensional, hydrodynamical simulations of the relativistic QNE impacting the dense degenerate WD under the settings described in this work, and couple the results with a nuclear network code to properly capture the relevant nucleosynthesis during WD burning and subsequent ablation. In particular these simulations would be important in assessing how much of the QN shock would pass through the WD and how much would go around it. Furthermore, a detailed study of how the spin-down energy is deposited and dissipated in the WD material remains to be done and its implications on the morphology of the light-curve should be shown. Finally, preliminary 1D simulations of the QN (Niebergal et al. 2010) indicate that our working hypothesis – the QN as a detonative transition from neutron to quark matter inside a NS – might be valid. If this is borne out by more sophisticated simulations, we will have found potentially a new engine for luminous (spin-down powered) sub-Chandrasekhar mass ($< 0.9\,M_{\odot}$) SNe-Ia plausibly hidden among observed SNe-Ia at high redshift. This highly speculative, but exciting, possibility should make our model for QNe-Ia (and the QN proper) worth pursuing.

**Acknowledgements** We thank P. Jaikumar, D. Welch, T. Tauris, J. Frank and B. Zhang for helpful discussions. We thank D. Leahy for comments on an earlier, letter version of this manuscript. The research of R. O. is supported by an operating grant from the National Science and Engineering Research Council of Canada (NSERC). This work has been supported, in part, by grant NNX10AC72G from NASA's ATP program.

## Appendix A: RELATIVISTIC SHOCK JUMP CONDITIONS

A shock is described by three jump conditions that express the continuity of mass, energy, and momentum flux densities, respectively, in the shock frame (Landau & Lifshitz 1959). When the QNE encounters the WD (i.e. a density jump $n_{\rm QNE}/\rho_{\rm WD}$), a reverse shock (RS) is driven into

[13] If one assumes that the observed type Ia SNe are a combination of DD and SD events, it would be quite a coincidence that most of the nearby, well-studied SNe-Ia had DD progenitors.

[14] The compact remnant (i.e. the QS) in the QN model is born as an aligned rotator (Ouyed et al. 2004; Ouyed et al. 2006), thus explaining why a radio pulsar has not been detected in this remnant.

the cold QNE, while a FS propagates into the cold higher density WD material. Therefore, there are four regions separated by the two shocks in this system: (1) unshocked cold WD matter, (2) forward-shocked hot WD matter, (3) reverse-shocked QNE and (4) unshocked cold QNE.

We denote $n_i$, $e_i$ and $p_i$ as the baryon number density, energy density and pressure of region "$i$" in its own rest frame respectively; $\Gamma_i$ and $\beta_i$ are the Lorentz factor and dimensionless velocity of region "$i$" measured in the local medium's rest frame respectively. The reverse- and forward-shock jump conditions simply state the conservation of energy, momentum, and particle number across the shock, which is equivalent to the continuity of their corresponding fluxes. We assume the EoSs for regions 2 and 3 to be relativistically hot and regions 1 and 4 to be cold. In regions 2 and 3 then $\rho_2 c^2 \ll p_2$ and $\rho_3 c^2 \ll p_3$ and the adiabatic index is $4/3$, implying $p_i = e_i/3 = w_i/4$; $w$ is the enthalpy. In region 1 we have $\rho_1 = w_1/c^2$, $p_1 = e_1 = 0$ and $\Gamma_1 = 1$ while region 4 describes the QNE. This leaves eight unknown quantities: $\Gamma$, $n$ and $e$ in regions 2 and 3, as well as the Lorentz factors of the reverse shock, $\Gamma_{\rm RS}$, and of the forward shock, $\Gamma_{\rm FS}$. Correspondingly, there are eight constraints: three from the shock jump conditions at each of the two shocks, and two at the contact discontinuity (pressure equilibrium and velocity equality along the contact discontinuity): $e_2 = e_3$ and $\Gamma_2 = \Gamma_3$. The equations describing the jump conditions for the FS become (Blandford & McKee 1976)

$$\frac{e_2}{n_2 m_p c^2} = \Gamma_2 - 1, \qquad \frac{n_2}{n_1} = 4\Gamma_2 + 3, \tag{A.1}$$

where $m_p$ is the proton mass. The relevant equations for the RS can similarly be derived.

Under the conditions specified above, the solution of the jump equations depends only on two parameters (e.g. Sari & Piran 1995): $\Gamma_4 = \Gamma_{\rm QNE}$ and $f = n_4/n_1 = n_{\rm QNE}/n_{\rm WD}$ (in our case $n_4 = n_{\rm QNE}$ is the number density of the QNE and $n_1 = n_{\rm WD}$ is the number density of the WD). The number density in the shocked WD (SWD) material/region is then $n_{\rm SWD} = n_2$ with $n_{\rm SWD}/n_{\rm WD}$ given in the equation above. In the co-moving frame of the "shocked" WD material (i.e. region 2) $n'_{\rm SWD} = \Gamma_2 n_{\rm SWD}$.

The Lorentz factor of the shocked WD material (i.e. region 2), $\Gamma_2$, can be shown to be

$$\Gamma_2 = \begin{cases} \Gamma_4 \ \text{ if } n_4/n_1 < \Gamma_4^2 \ , \\ (n_4/n_1)^{1/4}\Gamma_4^{1/2}/\sqrt{2} \ \text{ if } n_4/n_1 > \Gamma_4^2 \, . \end{cases} \tag{A.2}$$

When the RS is Newtonian ($n_4/n_1 < \Gamma_4^2$) it converts only a very small fraction of the kinetic energy into thermal energy; in this case the Lorentz factor of region 2 (the shocked WD material) relative to the rest frame of the WD (i.e. region 1; also an external observer) is $\Gamma_2 \simeq \Gamma_{\rm QNE}$. The relativistic RS limit ($n_4/n_1 > \Gamma_4^2$) is the regime where most of the kinetic energy of the QNE is converted to thermal energy by the shocks (in this case $\Gamma_2 \simeq (n_{\rm QNE}/n_{\rm WD})^{1/4}\Gamma_{\rm QNE}^{1/2}/\sqrt{2}$).

## References


Akerlof, C., Miller, J., Peters, C., et al. 2007, Central Bureau Electronic Telegrams, 1059, 2
Akmal, A., Pandharipande, V. R., & Ravenhall, D. G. 1998, Phys. Rev. C, 58, 1804
Alford, M., Rajagopal, K., & Wilczek, F. 1999, Nuclear Physics B, 537, 443
Alford, M., Blaschke, D., Drago, A., et al. 2007, Nature, 445, 7
Arnett, W. D. 1969, ApSS, 5, 180
Arnett, W. D. 1982, ApJ, 253, 785
Badenes, C., & Maoz, D. 2012, ApJ, 749, L11
Baldo, M., Bombaci, I., & Burgio, G. F. 1997, A&A, 328, 274
Bartunov, O. S., Tsvetkov, D. Y., & Filimonova, I. V. 1994, PASP, 106, 1276
Belczynski, K., & Taam, R. E. 2004, ApJ, 603, 690
Blandford, R. D., & McKee, C. F. 1976, Physics of Fluids, 19, 1130

Blondin, J. M., Chevalier, R. A., & Frierson, D. M. 2001, ApJ, 563, 806
Bodmer, A. R. 1971, Phys. Rev. D, 4, 1601
Branch, D., Buta, R., Falk, S. W., et al. 1982, ApJ, 252, L61
Branch, D., Lacy, C. H., McCall, M. L., et al. 1983, ApJ, 270, 123
Branch, D., Fisher, A., & Nugent, P. 1993, AJ, 106, 2383
Branch, D., Livio, M., Yungelson, L. R., Boffi, F. R., & Baron, E. 1995, PASP, 107, 1019
Bravo, E., García-Senz, D., Cabezón, R. M., & Domínguez, I. 2009, ApJ, 695, 1257
Carlberg, R. G., Yee, H. K. C., Lin, H., et al. 1998, Omega M and the CNOC Surveys, in Large Scale Structure: Tracks and Traces, eds. V. Mueller, S. Gottloeber, J. P. Muecket, & J. Wambsganss, 119
Chatzopoulos, E., Wheeler, J. C., & Vinko, J. 2012, ApJ, 746, 121
Chen, W.-C., & Li, X.-D. 2006, MNRAS, 373, 305
Chevalier, R. A., & Fransson, C. 1992, ApJ, 395, 540
Contopoulos, I., & Spitkovsky, A. 2006, ApJ, 643, 1139
Dan, M., Rosswog, S., Guillochon, J., & Ramirez-Ruiz, E. 2011, ApJ, 737, 89
Demorest, P. B., Pennucci, T., Ransom, S. M., Roberts, M. S. E., & Hessels, J. W. T. 2010, Nature, 467, 1081
Dessart, L., Burrows, A., Ott, C. D., et al. 2006, ApJ, 644, 1063
Dessart, L., Burrows, A., Livne, E., & Ott, C. D. 2007, ApJ, 669, 585
Dickinson, M., Papovich, C., Ferguson, H. C., & Budavári, T. 2003, ApJ, 587, 25
D'Souza, M. C. R., Motl, P. M., Tohline, J. E., & Frank, J. 2006, ApJ, 643, 381
Dursi, L. J., & Timmes, F. X. 2006, ApJ, 641, 1071
Eggleton, P. P. 1983, ApJ, 268, 368
Even, W., & Tohline, J. E. 2009, ApJS, 184, 248
Ferdman, R. D., Stairs, I. H., Kramer, M., et al. 2010, ApJ, 711, 764
Filippenko, A. V. 1997, ARA&A, 35, 309
Filippenko, A. V. 2003, in From Twilight to Highlight: The Physics of Supernovae, eds. W. Hillebrandt & B. Leibundgut (Berlin: Springer), 171
Fink, M., Hillebrandt, W., & Röpke, F. K. 2007, A&A, 476, 1133
Fink, M., Röpke, F. K., Hillebrandt, W., et al. 2010, A&A, 514, A53
Foley, R. J., Chornock, R., Filippenko, A. V., et al. 2009, AJ, 138, 376
Foley, R. J., Narayan, G., Challis, P. J., et al. 2010, ApJ, 708, 1748
Fryer, C., Benz, W., Herant, M., & Colgate, S. A. 1999, ApJ, 516, 892
Gamezo, V. N., Khokhlov, A. M., & Oran, E. S. 2005, ApJ, 623, 337
Gamezo, V. N., Wheeler, J. C., Khokhlov, A. M., & Oran, E. S. 1999, ApJ, 512, 827
González Hernández, J. I., Ruiz-Lapuente, P., Tabernero, H. M., et al. 2012, Nature, 489, 533
Hamuy, M., Phillips, M. M., Suntzeff, N. B., et al. 1996, AJ, 112, 2391
Hamuy, M., Trager, S. C., Pinto, P. A., et al. 2000, AJ, 120, 1479
Hayden, B. T., Garnavich, P. M., Kessler, R., et al. 2010, ApJ, 712, 350
Hicken, M., Garnavich, P. M., Prieto, J. L., et al. 2007, ApJ, 669, L17
Hoflich, P., Khokhlov, A. M., & Wheeler, J. C. 1995, ApJ, 444, 831
Höflich, P., Krisciunas, K., Khokhlov, A. M., et al. 2010, ApJ, 710, 444
Howell, D. A., Sullivan, M., Nugent, P. E., et al. 2006, Nature, 443, 308
Howell, D. A., Sullivan, M., Conley, A., & Carlberg, R. 2007, ApJ, 667, L37
Hoyle, F., & Fowler, W. A. 1960, ApJ, 132, 565
Hughes, D. H., Serjeant, S., Dunlop, J., et al. 1998, Nature, 394, 241
Hwang, U., & Laming, J. M. 2012, ApJ, 746, 130
Iben, I., Jr., & Tutukov, A. V. 1984, ApJS, 54, 335
Itoh, N. 1970, Progress of Theoretical Physics, 44, 291
Ivanova, N., & Taam, R. E. 2004, ApJ, 601, 1058
Iwamoto, K., Brachwitz, F., Nomoto, K., et al. 1999, ApJS, 125, 439

Iwazaki, A. 2005, Phys. Rev. D, 72, 114003
Jackson, A. P., Calder, A. C., Townsley, D. M., et al. 2010, ApJ, 720, 99
Jaikumar, P., Meyer, B. S., Otsuki, K., & Ouyed, R. 2007, A&A, 471, 227
Jordan, G. C., IV, Fisher, R. T., Townsley, D. M., et al. 2008, ApJ, 681, 1448
Kasen, D. 2006, ApJ, 649, 939
Kasen, D., & Bildsten, L. 2010, ApJ, 717, 245
Kasen, D., Röpke, F. K., & Woosley, S. E. 2009, Nature, 460, 869
Kepler, S. O., Kleinman, S. J., Nitta, A., et al. 2007, MNRAS, 375, 1315
Keränen, P., Ouyed, R., & Jaikumar, P. 2005, ApJ, 618, 485
Kerzendorf, W. E., Schmidt, B. P., Laird, J. B., Podsiadlowski, P., & Bessell, M. S. 2012, ApJ, 759, 7
Khokhlov, A. M. 1989, MNRAS, 239, 785
Khokhlov, A. M. 1991a, A&A, 245, 114
Khokhlov, A. M. 1991b, A&A, 245, L25
Kromer, M., Sim, S. A., Fink, M., et al. 2010, ApJ, 719, 1067
Kroupa, P., Famaey, B., de Boer, K. S., et al. 2010, A&A, 523, A32
Landau, L. D., & Lifshitz, E. M. 1959, Fluid mechanics (Oxford: Pergamon)
Landau, L. D., & Lifshitz, E. M. 1975, Course of Theoretical Physics – Pergamon International Library of Science, Technology, Engineering and Social Studies (Oxford: Pergamon Press), 1975, 4th rev.engl.ed.
Leahy, D., & Ouyed, R. 2008, MNRAS, 387, 1193
Leahy, D., & Ouyed, R. 2009, Advances in Astronomy, 2009, 306821
Lesaffre, P., Han, Z., Tout, C. A., Podsiadlowski, P., & Martin, R. G. 2006, MNRAS, 368, 187
Li, W., Filippenko, A. V., Treffers, R. R., et al. 2001, ApJ, 546, 734
Li, W., Filippenko, A. V., Chornock, R., et al. 2003, PASP, 115, 453
Livio, M. 2000, in Type Ia Supernovae, Theory and Cosmology, eds. J. C. Niemeyer & J. W. Truran (Cambridge: Cambridge Univ. Press), 33
Livne, E., & Glasner, A. S. 1990, ApJ, 361, 244
Livne, E., & Glasner, A. S. 1991, ApJ, 370, 272
Livne, E., & Arnett, D. 1995, ApJ, 452, 62
Livne, E., Asida, S. M., & Höflich, P. 2005, ApJ, 632, 443
Lorén-Aguilar, P., Isern, J., & García-Berro, E. 2009, A&A, 500, 1193
Madau, P., Pozzetti, L., & Dickinson, M. 1998, ApJ, 498, 106
Maeda, K., Tanaka, M., Nomoto, K., et al. 2007, ApJ, 666, 1069
Maeda, K., & Iwamoto, K. 2009, MNRAS, 394, 239
Maguire, K., Sullivan, M., Thomas, R. C., et al. 2011, MNRAS, 418, 747
McClelland, C. M., Garnavich, P. M., Galbany, L., et al. 2010, ApJ, 720, 704
Meakin, C. A., Seitenzahl, I., Townsley, D., et al. 2009, ApJ, 693, 1188
Meng, X., Chen, X., & Han, Z. 2008, A&A, 487, 625
Meng, X. C., & Yang, W. M. 2011, A&A, 531, A94
Milgrom, M., & Usov, V. V. 2000, ApJ, 531, L127
Muno, M. P., & Mauerhan, J. 2006, ApJ, 648, L135
Nelemans, G., Yungelson, L. R., van der Sluys, M. V., & Tout, C. A. 2010, MNRAS, 401, 1347
Niebergal, B., Ouyed, R., & Jaikumar, P. 2010, Phys. Rev. C, 82, 062801
Nomoto, K. 1982, ApJ, 257, 780
Nomoto, K., & Iben, I., Jr. 1985, ApJ, 297, 531
Nomoto, K., Umeda, H., Kobayashi, C., et al. 2000, in American Institute of Physics Conference Series, 522, Type Ia Supernovae: Progenitors and Evolution with Redshift, eds. S. S. Holt, & W. W. Zhang, 35
Nomoto, K., Saio, H., Kato, M., & Hachisu, I. 2007, ApJ, 663, 1269
Oemler, A., Jr., & Tinsley, B. M. 1979, AJ, 84, 985
Ouyed, R. 2012, MNRAS, in Press (arXiv: 1203.2703)

Ouyed, R., & Butler, M. 1999, ApJ, 522, 453
Ouyed, R., Dey, J., & Dey, M. 2002, A&A, 390, L39
Ouyed, R., Elgarøy, Ø., Dahle, H., & Keränen, P. 2004, A&A, 420, 1025
Ouyed, R., Rapp, R., & Vogt, C. 2005, ApJ, 632, 1001
Ouyed, R., Niebergal, B., Dobler, W., & Leahy, D. 2006, ApJ, 653, 558
Ouyed, R., Leahy, D., & Niebergal, B. 2007a, A&A, 473, 357
Ouyed, R., Leahy, D., & Niebergal, B. 2007b, A&A, 475, 63
Ouyed, R., Leahy, D., & Jaikumar, P. 2009, arXiv: 0911.5424
Ouyed, R., Staff, J., & Jaikumar, P. 2011a, ApJ, 729, 60
Ouyed, R., Staff, J., & Jaikumar, P. 2011b, ApJ, 743, 116
Ouyed, R., Leahy, D., Ouyed, A., & Jaikumar, P. 2011c, Physical Review Letters, 107, 151103
Ouyed, R., Kostka, M., Koning, N., Leahy, D. A., & Steffen, W. 2012, MNRAS, 423, 1652
Ouyed, R., & Leahy, D. 2009, ApJ, 696, 562
Ouyed, R., & Leahy, D. 2012, arXiv:1202.2400
Özel, F., Psaltis, D., Ransom, S., Demorest, P., & Alford, M. 2010, ApJ, 724, L199
Padmanabhan, T. 2001, Theoretical Astrophysics - Volume 2, Stars and Stellar Systems, ed. T. Padmanabhan (Cambridge Univ. Press)
Pakmor, R., Hachinger, S., Röpke, F. K., & Hillebrandt, W. 2011, A&A, 528, A117
Perlmutter, S., Aldering, G., Goldhaber, G., et al. 1999, ApJ, 517, 565
Pettini, M., Kellogg, M., Steidel, C. C., et al. 1998, ApJ, 508, 539
Pfahl, E., Rappaport, S., & Podsiadlowski, P. 2003, ApJ, 597, 1036
Pfannes, J. M. M., Niemeyer, J. C., & Schmidt, W. 2010, A&A, 509, A75
Phillips, M. M. 1993, ApJ, 413, L105
Phillips, M. M. 2012, PASA, 29, 434
Plewa, T. 2007, ApJ, 657, 942
Podsiadlowski, P., Rappaport, S., & Pfahl, E. D. 2002, ApJ, 565, 1107
Podsiadlowski, P., Mazzali, P., Lesaffre, P., Han, Z., & Förster, F. 2008, New Astron. Rev., 52, 381
Pritchet, C. J., Howell, D. A., & Sullivan, M. 2008, ApJ, 683, L25
Pskovskii, Y. P. 1969, Soviet Ast., 12, 750
Raskin, C., Scannapieco, E., Rhoads, J., & Della Valle, M. 2009, ApJ, 707, 74
Renzini, A. 1996, in IAU Colloq. 145: Supernovae and Supernova Remnants, eds. R. McCray & Z. Wang (Cambridge: Cambridge Univ. Press), 77
Riess, A. G., Press, W. H., & Kirshner, R. P. 1996, ApJ, 473, 88
Riess, A. G., Filippenko, A. V., Challis, P., et al. 1998, AJ, 116, 1009
Röpke, F. K., & Hillebrandt, W. 2004, A&A, 420, L1
Röpke, F. K., Gieseler, M., & Hillebrandt, W. 2005, in Astronomical Society of the Pacific Conference Series, 342, Supernovae as Cosmological Lighthouses, eds. M. Turatto, S. Benetti, L. Zampieri, & W. Shea, 397
Röpke, F. K., & Niemeyer, J. C. 2007, A&A, 464, 683
Rosswog, S., Ramirez-Ruiz, E., & Hix, W. R. 2009a, ApJ, 695, 404
Rosswog, S., Kasen, D., Guillochon, J., & Ramirez-Ruiz, E. 2009b, ApJ, 705, L128
Ruiter, A. J., Belczynski, K., & Fryer, C. 2009, ApJ, 699, 2026
Ruiter, A. J., Belczynski, K., Sim, S. A., et al. 2011, MNRAS, 417, 408
Saio, H., & Nomoto, K. 1985, A&A, 150, L21
Saio, H., & Nomoto, K. 2004, ApJ, 615, 444
Sari, R., & Piran, T. 1995, ApJ, 455, L143
Schaefer, B. E., & Pagnotta, A. 2012, Nature, 481, 164
Shapiro, S. L., & Teukolsky, S. A. 1983, Black Holes, White Dwarfs, and Neutron Stars: The Physics of Compact Objects (Wiley & Sons)
Sharpe, G. J. 1999, Journal of Fluid Mechanics, 401, 311

Shen, K. J., Bildsten, L., Kasen, D., & Quataert, E. 2012, ApJ, 748, 35
Sim, S. A., Röpke, F. K., Hillebrandt, W., et al. 2010, ApJ, 714, L52
Spergel, D. N., Verde, L., Peiris, H. V., et al. 2003, ApJS, 148, 175
Spruit, H. C., & Taam, R. E. 2001, ApJ, 548, 900
Staff, J. E., Ouyed, R., & Jaikumar, P. 2006, ApJ, 645, L145
Staff, J., Niebergal, B., & Ouyed, R. 2008, MNRAS, 391, 178
Staff, J. E., Jaikumar, P., Chan, V., & Ouyed, R. 2012, ApJ, 751, 24
Stairs, I. H. 2004, Science, 304, 547
Stritzinger, M., & Leibundgut, B. 2005, A&A, 431, 423
Stritzinger, M., Mazzali, P. A., Sollerman, J., & Benetti, S. 2006a, A&A, 460, 793
Stritzinger, M., Leibundgut, B., Walch, S., & Contardo, G. 2006b, A&A, 450, 241
Stritzinger, M. D., Phillips, M. M., Boldt, L. N., et al. 2011, AJ, 142, 156
Sullivan, M., Le Borgne, D., Pritchet, C. J., et al. 2006, ApJ, 648, 868
Sullivan, M., Conley, A., Howell, D. A., et al. 2010, MNRAS, 406, 782
Taam, R. E., & van den Heuvel, E. P. J. 1986, ApJ, 305, 235
Taam, R. E. 2004, in Revista Mexicana de Astronomia y Astrofisica Conference Series, 20, eds. G. Tovmassian, & E. Sion, 81
Tauris, T. M., van den Heuvel, E. P. J., & Savonije, G. J. 2000, ApJ, 530, L93
Tauris, T. M. 2011, in Astronomical Society of the Pacific Conference Series, 447, Evolution of Compact Binaries, eds. L. Schmidtobreick, M. R. Schreiber, & C. Tappert, 285
Tauris, T. M., Langer, N., & Kramer, M. 2011, MNRAS, 416, 2130
Terazawa, H. 1979, INS-Report-338, University of Tokyo (J. Phys. Soc. Japan, 58, 3555)
Timmes, F. X., Brown, E. F., & Truran, J. W. 2003, ApJ, 590, L83
Townsley, D. M., & Bildsten, L. 2004, ApJ, 600, 390
Tremblay, P.-E., & Bergeron, P. 2009, ApJ, 696, 1755
Uhm, Z. L. 2011, ApJ, 733, 86
Valenti, S., Pastorello, A., Cappellaro, E., et al. 2009, Nature, 459, 674
van den Heuvel, E. P. J. 2011, Bulletin of the Astronomical Society of India, 39, 1
van Kerkwijk, M. H., Chang, P., & Justham, S. 2010, ApJ, 722, L157
Vogt, C., Rapp, R., & Ouyed, R. 2004, Nuclear Physics A, 735, 543
Wang, B., Meng, X.-C., Wang, X.-F., & Han, Z.-W. 2008, ChJAA (Chin. J. Astron. Astrophys.), 8, 71
Wang, L., & Wheeler, J. C. 2008, ARA&A, 46, 433
Webbink, R. F. 1984, ApJ, 277, 355
Weissenborn, S., Sagert, I., Pagliara, G., Hempel, M., & Schaffner-Bielich, J. 2011, ApJ, 740, L14
Williams, B. J., Blair, W. P., Blondin, J. M., et al. 2011, ApJ, 741, 96
Witten, E. 1984, Phys. Rev. D, 30, 272
Woosley, S. E., Weaver, T. A., & Taam, R. E. 1980, in Texas Workshop on Type I Supernovae, ed. J. C. Wheeler (Austin, TX: Univ. Texas), 96
Woosley, S. E., & Weaver, T. A. 1986, ARA&A, 24, 205
Woosley, S. E., & Weaver, T. A. 1994, ApJ, 423, 371
Woosley, S. E., Heger, A., Cumming, A., et al. 2004, ApJS, 151, 75
Woosley, S. E. 2010, ApJ, 719, L204
Woosley, S. E., & Kasen, D. 2011, ApJ, 734, 38
Wright, E. L. 2006, PASP, 118, 1711
Xu, R. X. 2005, MNRAS, 356, 359
Yoon, S.-C., & Langer, N. 2005, A&A, 435, 967
Yoon, S.-C., Podsiadlowski, P., & Rosswog, S. 2007, MNRAS, 380, 933
Zhang, B., & Kobayashi, S. 2005, ApJ, 628, 315